PROCESS DEVELOPMENT FOR THE FABRICATION OF MESOSCALE ELECTROSTATIC VALVE ASSEMBLY

By

SHAILINI DHRU
Nirma Institute of Technology, 2004

A thesis submitted in partial fulfillment of the requirements
for the degree of Master of Science
in the School of Electrical Engineering and Computer Science
at the University of Central Florida
Orlando, Florida

Fall Term
2007

© 2007 Shailini Dhru

ABSTRACT

This study concentrates on two of the main processes involved in the fabrication of electrostatic valve assembly, thick resist photolithography and wet chemical etching of a polyamide film. The electrostatic valve has different orifice diameters of 25, 50, 75 and 100 µm. These orifice holes are to be etched in the silicon wafer with deep reactive ion etching. The photolithography process is developed to build a mask of 15 µm thick resist pattern on silicon wafer. This photo layer acts as a mask for deep reactive ion etching. Wet chemical etching process is developed to etch kapton polyamide film. This etched film is used as a stand off, gap between two electrodes of the electrostatic valve assembly. The criterion is to develop the processed using standard industry tools. Pre post etch effects, such as, surface roughness, etching pattern, critical dimensions on the samples are measured with Veeco profilometer.

Dedicated to My loving Parents.

ACKNOWLEDGMENTS

I would truly like to thank my advisor Dr Kalpathy B. Sundaram for making this a great learning opportunity. Despite his hectic schedule he made every effort possible to provide me with insightful guidance and support throughout this effort.

I would like to thank Dr. Parveen Wahid and Dr Xun Gong for serving on my thesis committee and giving me their valuable suggestions. I am highly grateful to Edward Dein and Ben Nguyenphu for giving me helpful suggestions at all times. I also wish to acknowledge Advanced Microfabrication Facility and the Materials Characterization Facility at the Advanced Materials Processing and Analysis Center for laboratory support. I appreciate former AMPAC director; Dr. Vimal Desai, for being kind and supportive. I would also like to express my appreciations to Ajith Kumar Balan and Ravi Peelamadu for their valuable help during my research work. Finally, I express my deepest gratitude towards my family and friends who supported me with their love for every moment during ups and downs of this work.

TABLE OF CONTENTS

LIST OF FIGURES viii

LIST OF TABLES ix

LIST OF ACRONYMS/ABBREVIATIONS x

CHAPTER 1: INTRODUCTION 1

CHAPTER 2: PROCESS DESIGN 6

2.1 Photolithography Process Design 12

2.1.1 Steps Involved in a Photolithography Process 13

2.1.2 AZ 4620 Positive Resist 15

2.1.3 AZ Developer 17

2.2 Deep Reactive Ion Etching 18

2.3 Kapton Polyamide 21

2.4 Surface Roughness Measurements 24

2.5 Standard Cleaning Process 1 and 2 (SC1 and SC2) 27

CHAPTER 3: EXPERIMENTS AND RESULTS 28

3.1 Photolithography Process with PR 4620 Positive Resist 28

3.1.1 Spin Speed and Time Variation 28

3.1.2 Exposure Time Variation 33

3.1.3 Bake Time Variation 38

3.2 Kapton Etching Methodology 42

3.2.1 Procedures for Kapton Etching 43

3.2.2 Post Etch Results 46

3.2.3 Surface Roughness and Etch Rate Measurement.. 49

CHAPTER 4: CONCLUSION 52

LIST OF REFERENCES 55

LIST OF FIGURES

Figure 2.1 Electro-statically Driven Actuator 7

Figure 2.2 Block Diagram of the valve fabrication process 8

Figure 2.3: (a) S shape (b) Cantilever valve configuration 9

Figure 2.4 Different conductance scenarios 11

Figure 2.5 Basic photolithography process 13

Figure 2.6 Spin speed vs. film thickness curve 16

Figure2.7 Performance of AZ P4620 Photoresist 17

Figure 2.8 Veeco Profilometer 25

Figure 3.1 Parameters measured in photolithography process 29

Figure 3.2 Veeco measurement for step height of photoresist 31

Figure 3.3 Spin speed vs. Resist thickness graph 33

Figure 3.4 Pattern diameter measurement for 72 sec exposure time 35

Figure 3.5 Pattern diameter measurement for 66 sec exposure time 36

Figure 3.6 Pattern diameter measurement for 60 sec exposure time 37

Figure 3.7 Exposure time vs. sidewall profile graph 38

Figure 3.8 Hump created with hard bake time 15 min 39

Figure 3.9 Hump created with the hard bake time 10 min 40

Figure 3.10 Hump created with hard bake time 5 min 40

Figure 3.11 Pre Etch surface roughness measurement on one sample 48

Figure 3.12 Post etch surface roughness measurement on one sample 49

Figure 3.13 Etch rate curve for kapton 50

LIST OF TABLES

Table 2.1 Flow controller requirements 10

Table 2.2 Different Valve Structures 10

Table 2.3 Features of AZ P4000 series photoresist 15

Table 2.4 Developer Concentration 18

Table 2.5 Operational differences between PSI and VSI measurement 26

Table 3.1 Veeco measurement data for different spin speeds 32

Table 3.2 Veeco measurement data for different exposure time 34

Table 3.3 Effect of hard bake time on hump height 39

Table 3.4 Post DRIE measurement 41

Table 3.5 Roughness measurement on the smooth and rough side of the Kapton piece before etching 44

Table 3.6 Etching solution concentration for Kapton etching 44

Table 3.7 Experiment Results: Etch rate measurement 47

Table 3.8 Average Etch rate and surface roughness results 48

Table 3.9 Comparison of results 50

LIST OF ACRONYMS/ABBREVIATIONS

Au	Gold, Aurum
BST	Barium Strontium Titanate
°C	Degree Celsius
DI Water	De-Ionized Water
DRIE	Deep Reactive Ion etching
K	Kelvin
PR	Photoresist
PSI	Phase Shifting Interferometry
SC1	Standard Cleaning 1
SC2	Standard Cleaning 2
Si	Silicon
Ti	Titanium
VSI	Vertical Scanning Interferomtry
μm	Micrometer

CHAPTER 1: INTRODUCTION

Electrostatic valves are increasingly used in cryogenic cooler applications. These valves have various advantages over different other types of valves, such as, piezoelectric valves or thermo pneumatic valves. The comparison between different types of valves is shown in Table 2.2. Also passive coolers have been used for many years in space science applications due to their relatively high reliability and low vibration levels [1]. However, these are now joined by coolers requiring input power, also called as active devices or cryogenic coolers. Cryogenic coolers use closed thermodynamic cycles to transport heat up a temperature gradient to achieve lower cold end temperatures at the cost of electrical input power. The major types of cryogenic coolers are described below.

1. **Stirling cycle.** These coolers are based on causing a working gas to undergo a Stirling cycle which consists of two constant volume processes and two isothermal processes. Devices consist of a compressor pump and a displacer unit with a regenerative heat exchanger, known as a `regenerator'. Stirling cycle coolers were the first active cooler to be used successfully in space and have proved to be reliable and efficient. Recent years have seen the development of two-stage devices which extend the lower temperature range from 60-80K to 15-30K.
2. **Pulse tube.** Pulse tube coolers are similar to the Stirling cycle coolers although the thermodynamic processes are quite different. They consist of a compressor and a fixed regenerator. Since there are no moving parts at the cold-end, reliability is theoretically higher than Stirling cycle machines. Efficiencies approaching Stirling cycle coolers can be achieved.

3. **Joule-Thompson.** These coolers work using the Joule-Thomson (Joule-Kelvin), effect. A gas is forced through a thermally isolated porous plug or throttle valve by a mechanical compressor unit leading to isenthalpic (constant enthalpy) cooling. Although this is an irreversible process, with correspondingly low efficiency, J-T coolers are simple, reliable, and have low electrical and mechanical noise levels.
4. **Sorption.** Sorption coolers are essentially J-T coolers which use a thermo-chemical process to provide gas compression with no moving parts. Powdered sorbent materials (e.g. metal hydrides), are electrically heated and cooled to pressurize, circulate, and adsorb a working fluid such as hydrogen. Efficiency is low but may be increased by the use of mixed working gases. Demonstration models have already been flown and they are expected to be useful in long-life missions where very low vibration levels are required.
5. **Reverse Brayton.** Reverse/Turbo Brayton coolers have high efficiencies and are practically vibration free. Coolers consist of a rotary compressor, a rotary turbo-alternator (expander), and a counter flow heat exchanger (as opposed to the regenerator found in Stirling or Pulse Tube coolers). The compressor and expander use high-speed miniature turbines on gas bearings and small machines are thus very difficult to build. They are primarily useful for low temperature experiments (less than 10K), where a large machine is inevitable or for large capacity devices at higher temperatures (although these requirements are quite rare). A recent application of this class of cooler was the Creare device used to recover the NICMOS (Near Infrared Camera and Multi-Object Spectrometer) instrument on the Hubble Space Telescope.
6. **Adiabatic Demagnetization.** Adiabatic Demagnetization Refrigeration (ADR) has been used on the ground for many years to achieve milli-Kelvin temperatures after a first stage

cooling process. The process utilizes the magneto-caloric effect with a paramagnetic salt. These coolers are currently under development for space use.

7. **He coolers.** In addition to its use as a stored cryogenic liquid, the properties can be used to achieve temperatures below 1K with closed cycle "Sorption coolers" (above 250mK), and dilution refrigerators (above 50mK). The former are scheduled for use in the SPIRE and PACS instruments aboard the Hershel satellite whereas the latter will be used on the Planck mission.
8. **Optical cooling.** In recent years, the principle of optical cooling has been developed and demonstrated. The principle of anti-Stokes fluorescence in Ytterbium doped Zirconium Fluoride is used to provide vibration-free solid-state cooling. The principles of this technique are being developed and it will be many years before they are ready for space applications.
9. **Peltier effect coolers.** Solid-state Peltier coolers, or Thermo-Electric Converters (TECs), are routinely used in space to achieve temperatures above 170K (e.g. the freezers aboard the International Space Station). These devices work on the same principle as the Seebeck effect, but in reverse: the creation of a temperature difference between two dissimilar metals by application of a current. [2]

Typical temperature range for a pulse tube cryogenic cooler is 50K to 80K. The main advantage is it has very less vibrations and high efficiency. NASA used the pulse tube cryogenic cooler in their EOS/AIRS mission at the temperature 55K with a lifetime of 50,000 hours.

Pulse tube cryogenic cooler is a developing technology. It has been used extensively in industrial applications such as semiconductor fabrication and in military applications such as cooling of infrared sensors. Micro-fluid devices such as micro-valves and micro-pumps are

expected to minimize the size and dead space in gas control systems. The larger dead space results into a delay of several seconds to exchange the gases in the chamber. [3]

There is a strong interest in pulse tube cryogenic coolers for strategic applications. This interest is driven by the reliability inherent in a cryogenic cooler expander design in which traditional moving mechanical components have been eliminated. The pulse tube cryogenic cooler derives its thermodynamic performance from a controlled movement of a gas volume within a tube resulting in extraction of heat from a definable cold interface. Performance of pulse tube cryogenic coolers is strongly dependent on accurate control of the gas flow to achieve a matching of the moving gas volume with the tube volume and effective phasing of the gas volume motion relative to driving pressure waveforms. Performance of pulse tube cryogenic coolers is degraded by excessive gas volume within the working volume (gas between the compressor pistons and the interface to be cooled by the pulse tube). Non-functional volume within the working volume is referred to as dead volume.

Present pulse tube technology relies on flow control that is achieved using fixed geometry, e.g., fixed flow restrictor orifices or long, small diameter flow lines. Either approach relies on setting or selecting the flow restriction prior to operation of the pulse tube expander. A change in flow restriction requires some degree of physical disassembly of the expander for access to the restrictor. Neither approach lends itself to dynamic control of this flow restriction. A lack of dynamic controllability will also restrict the user to optimization for a specific operating regime; e.g. maximum cooling capacity for fast cool down or peak operating efficiency for steady state power conservation [4].

A second issue associated with present pulse tube flow control technology is the inherent coarseness of flow control. For proper operation, peak flow rates in the range of 10-50 mg/sec atm at pressure ratios of 1.2 to 1.5 are typical. At these flow rates, small changes in the flow

control device can result in relatively large changes in flow. In those cases in which length modifications can be made, flow control can be established as accurately as the flow restrictor length can be controlled; however, for those designs in which length is not variable, the flow control must be established by changing orifice area. A 10% change in effective diameter (which may be challenging for small orifices) will result in approximately a 20% change in effective orifice area [13]. A major benefit of a controllable micro-miniature flow manifold is dynamic control of the flow restrictor performance with minimal addition of parasitic void volume. The proposed approach is to ultimately package multiple electrostatic controlled flow valves that can be individually controlled throughout the pulse tube thermodynamic cycle for maximum performance flexibility.

CHAPTER 2: PROCESS DESIGN

An electro-statically driven micro-valve actuator structure is shown in Fig. 2.1. It consists of a pair of fixed electrode plates with a flexible conductive film between them. Each electrode is an electro-static component formed has an insulation layer on its surface and the cross section of the middle part of the film is elastically bent in S-shape. Both sides of this S-bend maintain contact with the electrode plates. When a voltage is applied between the film and the upper electrode, the electrostatic driving force works on the edge of the S-bend. [3] As a result, the S-bend propagates to the left side, increasing the contact area between the film and the upper electrode. It moves in the reverse direction when the voltage is applied between the film and the opposite electrode. Therefore, the S-bend moves back and forth by switching the applied voltage. An advantage of this actuator is that it allows vertical displacement of the film to the order of several hundred micrometers by increasing the spacing between the two electrode plates; this is because even if the spacing increased, electrostatic force works effectively at the edge of the S-shape maintained during operation. This actuator is, therefore, suitable for gas-control system requiring a large opening displacement to obtain a high gas-flow rate under low pressure conditions [4].

In fig. 2.1 [3] the conductive film is Titanium (Ti) and gold (Au) metal thin films. The insulation layer is barium strontium titanate (BST) and aluminum oxide (Al_2O_3) film. BST is used for its very high dielectric constant. Al_2O_3 has a very high dielectric breakdown voltage value. Thus BST and Al_2O_3 together forms an excellent capacitor required for the electrostatic valve [5]. The substrate used is double sided polished silicon wafer. Kapton polyamide film is

used as a flexure that forms the S shape. Also the kapton film is used as a stand off (vertical displacement between two electrodes. Stand off is 100 μm in height.

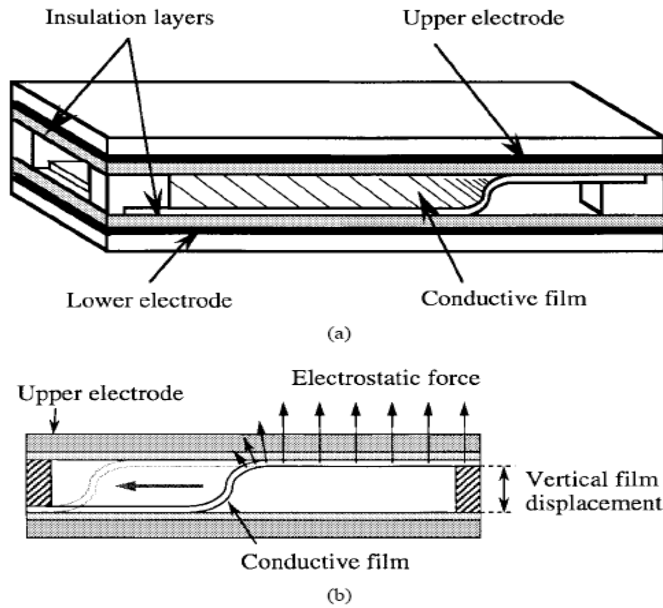

Figure 2.1 Electro-statically Driven Actuator

For electrode formation, 500 Å of Ti and Au are evaporated on one of the sides of double side polished silicon wafer. The insulation layer is made of BST and Al_2O_3. The vertical displacement film or also called stand off is made of Kapton polyamide. The work included in this thesis is uniform etching of Kapton polyamide film using wet chemistry, photolithography process development to build a 15 μm thick mask on silicon for deep reactive ion etching process used to etch valve holes in silicon.

The fabrication process is to be followed as described in the block diagram in Figure 2.2.

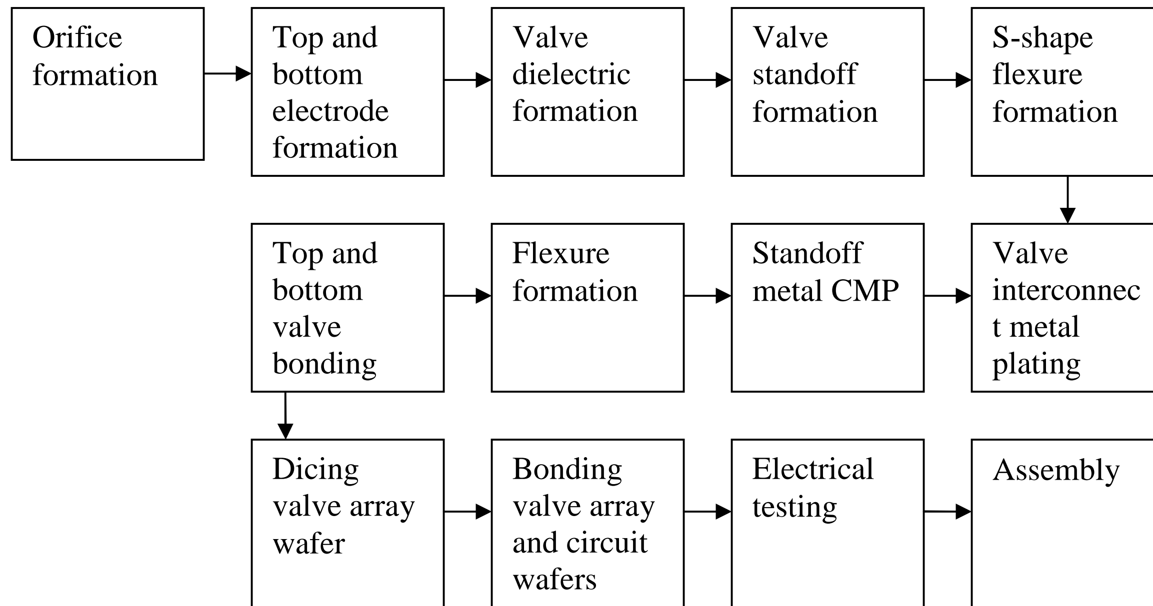

Figure 2.2 Block Diagram of the valve fabrication process

Experimental valve work has revealed two different configurations for the attachment of the flexure in the valve assembly: the original "s" configuration and a cantilever configuration where the thin flexure material is attached at only one end. An advantage of cantilever configuration is that material stiffness within flexure is not s limiting of a factor as in the "s" configuration. Fig. 2.3 displays each valve configuration in open and closed positions. A dynamic analysis of the flexure will enable scaling predictions to determine the smallest electrostatic valves that may be assembled before flexure stiffness overcomes electrostatic actuation.

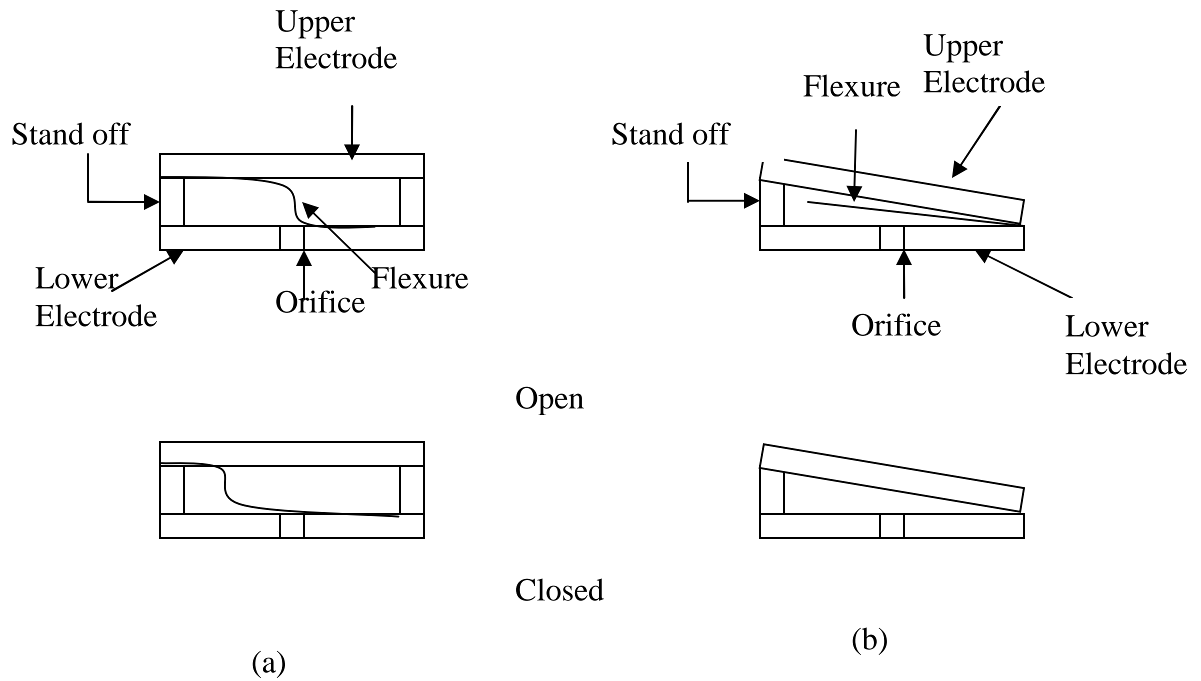

Figure 2.3: (a) S shape (b) Cantilever valve configuration

High efficiency and long life characteristics of the pulse tube cryogenic cooler are benefited by phase shift of oscillating pressure and mass flow. Current technology implements fixed orifice or interface tube to impart phase shift on the high density gas flow [4].

Purpose of phase shifter is to increase isentropic expansion of oscillating flow through pulse tube. Flow controller intends to increase pressure-volume envelope with minimum input power. Table 2.1 lists the flow controller requirements and Table 2.2 compares different valve structures.

Table 2.1 Flow controller requirements

PARAMETER		REQUIREMENT
Working Fluid		Helium
Pressure		20 to 45 atm
Heat rejection temperature		300 K
Operating temperature	Minimum	20 K
	Maximum	325 K

Table 2.2 Different Valve Structures

VALVE TYPE	FLOW CONDUCTANCE	ADVANTAGES	DISADVANTAGES	POWER DENSITY J/m^3
Electrostatic	High	High frequency operation	Stress on flexure	4×10^5
Bimetallic	Low	High frequency operation	Residual deflection	107
Thermo-pneumatic	Low	High flow resolution	No cryogenic application, slow actuation	4×10^7
Piezoelectric	Low	High frequency operation	Limited duty	105
Electromagnetic	High	High flow resolution	Low flow rate	106

From table 2.2 it can be seen that compared to other types of valve structures, electrostatic valve gives higher flow rate, better working condition at cryogenic temperatures, higher efficiency and longer lifetime due to less number of moving parts and hence less friction.

Figure 2.4 below describes the flow in different open/close valve conditions.

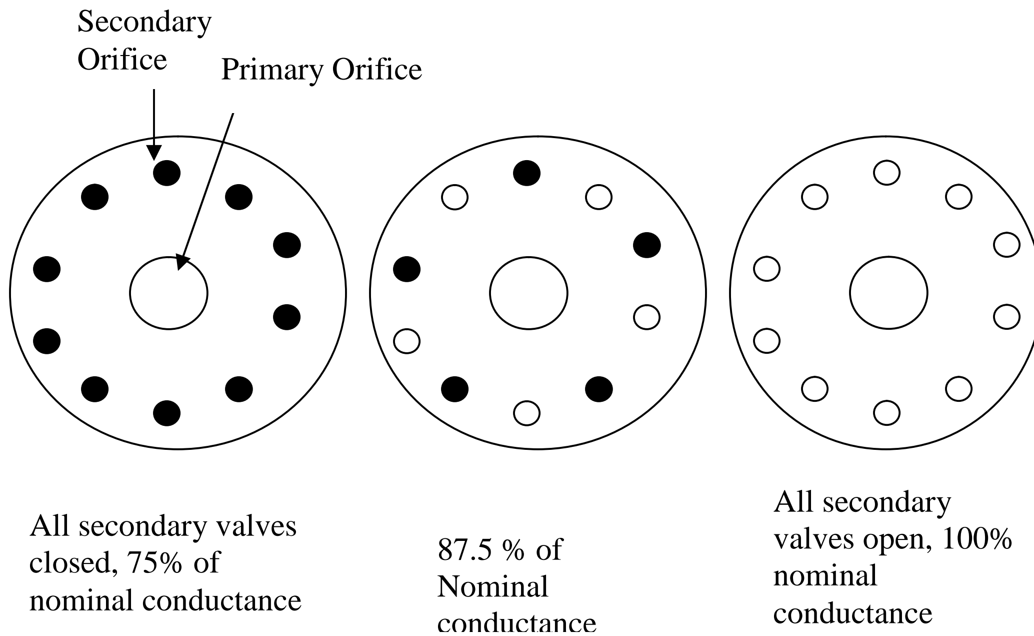

Primary valve size: 100 µm

Secondary valve size: 20 µm, 50 µm and 75 µm

Figure 2.4 Different conductance scenarios

Figure 2.4 also shows the pattern that needs to be etched in a 350 µm thick 3" silicon wafer. Deep reactive ion etching is used to etch through holes into silicon wafer. The mask used for DRIE process is the thick resist mask. This thesis concentrates on two of the main steps involved in fabrication of S shape actuator. First is photolithography, which is done to prepare a 15 µm thick photoresist mask on silicon wafer. The pattern of the photoresist is the different

valve sizes, 25 μm, 50 μm, 75 μm and 100 μm that need to be etched in Si using deep reactive ion etching technique. Since the resist thickness is very high, the areas of concern are baking time and exposure time to achieve a strait walled pattern. The second very important part is etching the polyamide film to desired thickness for the stand offs. Here the aim is to achieve a highly uniform smooth surface after the etch.

2.1 Photolithography Process Design

Photolithography is a process used in microfabrication to selectively remove parts of a thin film. The technique uses light to transfer a geometric pattern from a photo mask to a light sensitive chemical, known as photoresist, on the substrate. A series of chemical treatments then engraves the exposure pattern into the material underneath the photoresist. The main advantage of a photolithography technique is that it can give exact control over the shape and size of the objects it creates and also it can create the pattern over an entire surface simultaneously. There are two types of resists, positive and negative. For positive resist, the resist is exposed with UV light wherever the underlying material is to be removed. Exposure to UV light changes the chemical structure of positive resist such that it becomes more soluble in the developer. The exposed resist is then washed away by the developer solution, leaving windows of the bare underlying material as shown in Figure 2.5(a). The mask therefore contains an exact copy of the pattern which is to remain on the wafer.

Negative resist behaves in just the opposite manner. Exposure to UV light causes the negative resist to become polymerized and more difficult to dissolve. Therefore, the negative resist remains on the surface wherever it is exposed, and the developer solution removes the unexposed portions as shown in Figure 2.5(b). Masks used for negative photoresist contain the

inverse of the pattern to be transferred. The figure 2.5 below shows the differences generated from the use of positive and negative resist. [6]

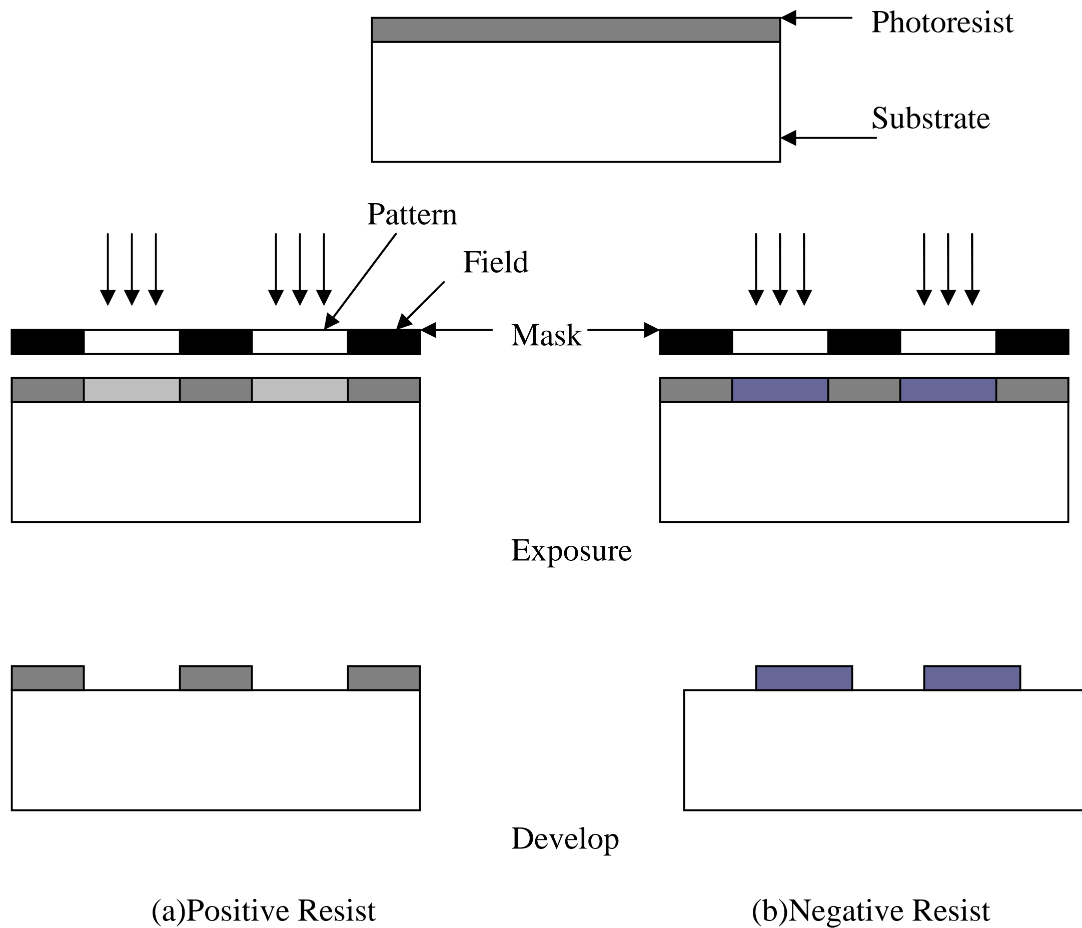

Figure 2.5 Basic photolithography process

2.1.1 Steps Involved in a Photolithography Process

Steps involved in any photolithography process are described below.

Coating: The resist is first applied on the substrate. Mostly the resist is in liquid form which is applied on the substrate surface through spin coating. First a substrate is centered on a vacuum

chuck. The substrate should be centered properly so that it does not wobble while spinning. Photoresist is put on the center of the substrate and then the substrate is spun at the speed of 1000-3000 rpm for 30-60 seconds (depending on the required thickness of the resist). The resist, while spinning, goes through change in colors when observed closely. When the resist is coated uniformly on the wafer the change in the color stops. After this even if the wafer is kept spinning on the vacuum chuck, there would be no change in the resist thickness. Thus, mainly the spin speed determines the thickness of the resist on a substrate. [7]

After the substrate is uniformly coated with photoresist, the sample is then put inside the oven for soft baking. This step enhances the adhesion of resist to the substrate surface and prepares the resist for exposure. After the soft baking step, it is required for the sample to reach the room temperature by natural cooling. Once it is cooled, photoresist is then exposed to UV light using mask aligner. After the exposure photoresist is developed in the developer solution. Developing time also depends on the resist thickness and the exposure time. After developing the sample is rinsed with DI water in order to remove residues of developer solution and then blow dried with N_2 gun. After developing, the sample is inspected under microscope to check if the pattern is properly developed or not. If the pattern is not developed completely, the sample is again immersed into the developer solution and developed for some more time, till the pattern is completely developed. And the last step is hard baking. This further enhances the bonding between the resist and the substrate. For the negative resist post exposure bake (PEB) is involved before the resist is developed. The objective of the PEB is to activate the photo-acid produced during the exposure, which, in a self-catalyzing sequence, attacks the bonds of the organic compounds within the resist, making them soluble to the developer solution. This sequence generates more photo-acid, and the cycle continues until the process self-quenches.

In this thesis, the thickness requirement of resist is 15 µm. And a pattern of strait-walled 100 µm, 75 µm, 50 µm and 25 µm holes has to be developed. Hence, the spin speed and time, bake time and temperature, exposure time and developing time have to be varied to meet the requirement. Pattern developed on the resist is different valve sizes that need to be etched in the silicon wafer. Hence the thickness is required for the deep reactive ion etching purposes.

2.1.2 AZ 4620 Positive Resist

AZ P4000 series photoresists offer unmatched capabilities in demanding applications requiring film thicknesses ranging from 3 to over 60 µm. The main features and benefits of AZ P4000 are listed in Table 2.3. [8]

Table 2.3 Features of AZ P4000 series photoresist

FEATURES	BENEFITS
Steep wall profiles and excellent adhesion on a wide variety of substrates	Ideal for up plating No underplating even in thick films
Sensitive to g-,h-, and i-line wavelengths	Sensitive to all popular exposure tools
Available in viscosities that allow coating thickness greater than 60 µm	Single resist series that can be used in a wide range of applications
Excellent ion-milling properties	High yields No cracking, peeling, or bubbling
Exceptionally stable cured films	Provides an excellent, easy to use permanent insulator layer for critical high reliability applications

Fig 2.6 [8] shows the spin speed vs. resist thickness curve for AZ P4903, AZ P4620 and AZ P4330 resists. It is clearly seen from the graph that P4330 gives a maximum thickness of 10 µm at the speed of 1000 rpm. With AZ P4903 the minimum thickness achieved is close to 15 µm or higher for a speed of 4000 rpm. AZ P4620 gives a maximum thickness of 40 µm and a minimum thickness of 10 µm. P4620 is a good choice for this frame of work as we need a 15 ± 1 µm thick resist.

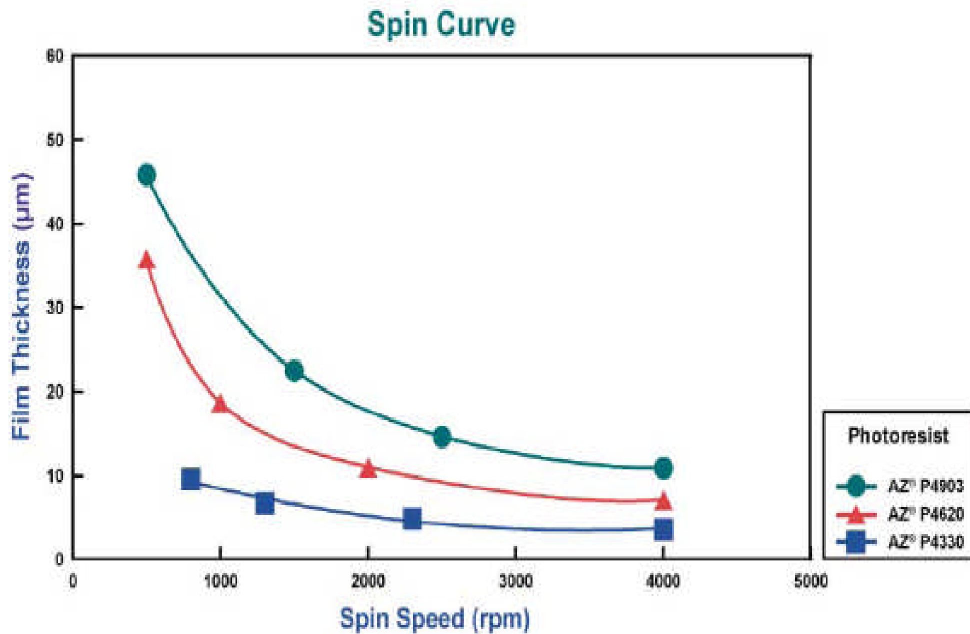

Figure 2.6 Spin speed vs. film thickness curve

Fig 2.7 [8] shows the linearity of developed pattern on Silicon with respect to the pattern on the mask. It can be clearly seen that the resist gives almost linear results in a higher offset region.

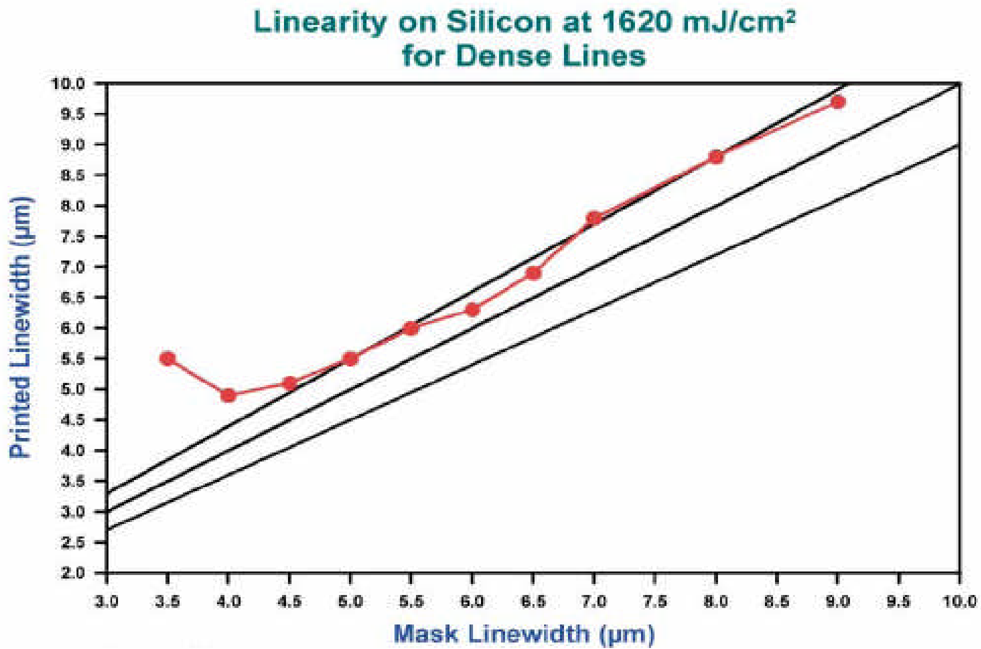

Figure2.7 Performance of AZ P4620 Photoresist

2.1.3 AZ Developer

AZ 400K developer is a potassium based buffered developer that provides optimal process control while minimizing contaminations risks by using the less mobile potassium ion. It provides high throughput and contrast, particularly for thick film photoresists. Developers typically have a limited range of useful dilutions. Highly concentrated dilutions have high sensitivity and allow faster photospeeds, but they are limited by high dark film losses and reduced contrast. The more dilute concentrations enable high contrast and provide greater selectivity between the exposed and unexposed resist. These require longer development time or increased exposure energy. They also have greater sensitivity to the effects of standing waves from monochromatic exposure. Table 2.4 shows different ratios that can be used for developing AZ resist. [9]

Table 2.4 Developer Concentration

Developer	High Sensitivity*	High Contrast*
AZ® Developer	2:1	1:1
AZ® 400K Developer	1:3	1:4

**developer:DI water*

The purpose of the experiment is to develop a 15 µm thick photoresist layer on a Silicon wafer and pattern it for Deep Reactive Ion Etching process. The pattern needs to be etched into the silicon wafer using DRIE technique. In order to have a uniform etching, the sidewalls of the thick resist pattern should be vertical and the critical dimensions of the pattern should not differ by ±1.5 µm.

The wafer used for this experiment is double sided polished 3" silicon wafer. Thickness of the wafer is 350 µm.

2.2 Deep Reactive Ion Etching

Deep reactive ion etching is a highly anisotropic etch process used to create deep, steep-walled holes and trenches in wafers, with aspect ratio of 20:1 or more.

Aspect ratio of an image is its width divided by its height.

There are two main technologies for high rate DRIE;

1. Cryogenic
2. Bosch

Both processes can fabricate 90° walls, but often the walls are slightly tapered, e.g. 88° or 92°.

In reactive ion etching (RIE) the substrate is placed inside a reactor in which several gases are introduced. Plasma is generated in the gas mixture using an RF power source. This breaks the gas molecules into ions. The gas ions are accelerated towards the surface of the material being etched and react with the surface to form another gaseous material. This is the chemical part of the RIE. In the physical part, the ions with high energy strike the material to be etched and knock the atoms out of the material without any chemical reaction.

Deep reactive ion etching is a subclass of reactive ion etching technique. With DRIE depths of hundreds of microns can be etched with almost vertical sidewalls. The primary technology is based on the Bosch process. [6]

Bosch process

In this process two different gas compositions are alternated in the reactor. The first gas composition creates a polymer on the surface of the substrate, and the second gas composition etches the substrate. The polymer is immediately sputtered away by the physical part of the etching, but only on the horizontal surfaces and not the sidewalls. Since the polymer only dissolves very slowly in the chemical part of the etching, it builds up on the sidewalls and protects them from etching. As a result etching aspect ratio of 50:1 can be achieved. The process can easily be used to etch completely through a silicon substrate and etch rates are 3-4 times higher than wet etching.

1. A standard, nearly isotropic plasma etch. The plasma contains some ions, which attack the wafer from a nearly vertical direction. (For silicon, this often uses sulfur hexafluoride [SF_6].)
2. Deposition of a chemically inert passivation layer. (For instance, C_4F_8 source gas yields a substance similar to Teflon.)

Each phase lasts for several seconds. The passivation layer protects the entire substrate from further chemical attack and prevents further etching. However, during the etching phase, the directional ions that bombard the substrate attack the passivation layer at the bottom of the trench (but not along the sides). They collide with it and sputter it off, exposing the substrate to the chemical etchant.

These etch/deposit steps are repeated many times over resulting in a large number of very small isotropic etch steps taking place only at the bottom of the etched pits. To etch through a 500 µm silicon wafer, for example, 100-1000 etch/deposit steps are needed. The two-phase process causes the sidewalls to rise and fall with an amplitude of about 100-500 nm. The cycle time can be adjusted with short cycles yielding smoother walls, and long cycles yielding a higher etch rate.

Another mechanism is sidewall passivation. Here SiO_xF_y functional groups (which originate from sulphur hexafluoride and oxygen etch gases) condensate on the sidewalls, and protect them from lateral etching. As a combination of these processes deep vertical structures can be made.

Cryogenic process

In cryo-DRIE, the wafer is chilled to -110°C (163 K). The low temperature slows down the chemical reaction that produces isotropic etching. However, ions continue to bombard upward-facing surfaces and etch them away. This process produces trenches with vertical sidewalls. [10]

2.3 Kapton Polyamide

Kapton® is a polyamide film developed by DuPont which has a wide variety of applications at temperatures as low as -269°C (452°F) and as high as 400°C (752°F). There are various types of Kapton tapes made for different applications. A brief description is given below. HN film can be laminated, metallized, punched, formed or adhesive coated. Kapton® HN is the recommended choice for applications that require an all-polyimide film with an excellent balance of properties over a wide range of temperatures. [11]

Kapton is used in various mechanical parts, electronic parts, electrical insulation, pressure sensitive tapes, fiber optic cables, insulation blankets, insulating tubing, automotive diaphragms sensors and manifolds and substrate for flexible printed circuits. The wide variety of applications are possible due to some of the great properties like excellent dielectric strength, very good dielectric dissipation factor, resistant to wide temperature range, chemical resistance at elevated temperatures and radiation resistance at elevated temperatures.

There are various types of Kapton available in the market and each film possesses a unique combination of properties. While most properties of Kapton® HN and HA are similar, there are a few slight differences which are listed below.

- Kapton® 100HN and Kapton® 100HA are made from the same polymer. The difference in properties is due to the manufacturing process only.
- Kapton® HA is a little lighter in color. This type of film is approximately 6 L-color units higher than Kapton® HN, which gives it a lighter appearance.

Characteristics

- Excellent hydrolysis resistance

- High dielectric strength
- Tough
- Heat fusible

Constructions/Packaging

Kapton® HA is available up to a maximum width of 48 in (1218 mm). Standard width is 24 in (609 mm). Kapton® HN is available up to a maximum width of 52 in (1320 mm). Standard width is 26 in (660 mm). Standard roll length is 5000 ft (1524 m) or 10,000 ft (3048 m). All packaging materials are 100% recyclable.

Storage Conditions/Shelf Life

Proper storage of Kapton® film will ensure its performance. Kapton® HA and HN should not be exposed to ultraviolet radiation as from direct sunlight or in conditions of high humidity for extended periods of time. The storage life will be decreased dramatically under these conditions. The shelf life for Kapton® in typical warehouse temperature will be in excess of 20 years. Rolls should be kept wrapped in storage to prevent surface contamination.

Safe Handling

Proper care should be taken when handling Kapton® polyimide film. Processing at high temperatures requires adequate ventilation and air circulation. Scrap film should be disposed of in a landfill. Some basic properties of different types of Kapton are described below.

Kapton® BCL-Y: Kapton® BCL-Y is a two-sided, printable, homogeneous film that possesses excellent hydrolytic and chemical durability.

Kapton® CR: Developed specifically to withstand the damaging effects of corona and can easily handle high voltage stress environments.

Kapton® FCR: Withstands corona discharge while delivering improved long-term performance for motors and generators. [11]

Kapton® FN: Kapton® FN is a general purpose HN film that is coated or laminated on one or both sides with Teflon® FEP fluoropolymer. Kapton® FN imparts heat sealability, provides a moisture barrier, and enhances chemical resistance.

Kapton® FPC: Kapton® FPC is the same tough polyimide as Kapton® VN film, but has improved bondability for use in the flexible printed circuit market.

Kapton® HN: A general-purpose film that has been used successfully in applications at temperatures as low as -269°C (-452°F) and as high as 400°C (752°F).

Kapton® HPP-ST : A two-sided, treated film that offers the same excellent balance of physical, chemical, and electrical properties over a wide temperature range offered by general purpose Kapton® HN.

Kapton® MT : Kapton® MT polyimide film is a homogeneous film possessing 3x the thermal conductivity and cut-through strength of standard Kapton® HN.

Kapton® PST: Kapton® PST grade polyimide film is a crystalline film designed for the pressure sensitive tape industry with improved film attributes for PST coaters.

Kapton® CB: Kapton® CB is an opaque, black substrate film offering low light transmission, reflectivity and superior durability.

Kapton® E: Kapton® E is a premium performance polyimide film and is used as a dielectric substrate for flexible printed circuits and high density interconnects.

Kapton® FWR: Kapton® FWR films are polyimide-FEP fluoropolymer substrate materials that provide tough, high dielectric strength insulation with improved hydrolysis resistance, compared to other commonly used polyimide-containing materials. [11]

Kapton® MTB: Kapton® MTB polyimide film is a black, homogeneous product with increased thermal conductivity over Kapton® HN. It has excellent adhesion properties, making it compatible with difficult adhesion applications.

Kapton® V: Kapton® V is recommended for applications that require a smooth surface and superior dimensional stability.

Kapton® VN: The same tough polyimide film as Kapton® HN Film, with superior dimensional stability at elevated temperatures. For applications requiring low shrinkage properties, Kapton® VN is an excellent choice.

Kapton® XC: Kapton® XC polyimide films have proven performance in numerous satellite applications where it provides both thermal and anti-static control.

For this thesis work, general purpose Kapton HN type sheet is selected. Kapton HN sheet can handle wide range of temperature so it becomes the first choice for the electrostatic valve actuator which has to be used at cryogenic temperatures.

2.4 Surface Roughness Measurements

Surface roughness measurement is an important factor in determining reliability of the etched samples. The surface profilometry was done using VEECO NT3300 Optical profilometer. The NT3300 is a non-contact surface profiler which was used to measure the surface roughness of the etched samples. This profilometer uses two different technologies to measure a wide variety of surface heights. Phase shifting interferometry (PSI) is reliable for smooth surfaces and small steps in which the height change between two adjacent points is not more than 160 nm. The vertical resolution for PSI mode is 3Å for a single measurement and 1Å for multiple

averaged measurements. Vertical scanning interferometry (VSI) allows measurement of rough surface profiles and steps up to few millimeters high. The vertical resolution is 3nm for a single measurement and <1nm for averaged multiple measurements. Figure 2.8 is a picture of NT3300 veeco profilometer. [12]

Figure 2.8 Veeco Profilometer

The roughness measurements were made in both VSI and PSI mode at a resolution using a 5X objective. The profilometer was calibrated using the mirror calibration sample before

measurements were taken. Several measurements were made to check the accuracy of measurements.

Table 2.5 [12] describes the two types of measurement techniques used by Veeco profilometer.

Table 2.5 Operational differences between PSI and VSI measurement

Vertical Scanning Interferometry	Phase Shifting Interferometry
Neutral Density filter for white light	Narrow bandwidth filtered light
Vertically scans- the objective actually moves through the focus	Phase-shift at a single point-the objective does not move.
Processes fringe modulation data from the intensity signal to calculate surface heights.	Processes phase shift data from the intensity signal to calculate surface heights
Primarily used to measure step heights	Primarily used to measure roughness of the films

The average roughness and peak to valley roughness was measured for all the etched samples. Average roughness (R_a) represents the two dimensional roughness averages, the arithmetic mean of the absolute values of the surface departures from the mean plane. where M and N are the number of data points in the X and Y direction, respectively of the array and Z is the surface height relative to the surface reference mean plane.

$$R_a = \frac{1}{MN} \sum_{j=1}^{M} \sum_{i=1}^{N} \left| Z_{ji} \right|$$

Peak to valley roughness (R_t), the maximum height of the surface is the vertical distance between the highest (R_p) and lowest (R_v) points as calculated over the entire dataset.

$R_t = R_p + R_v$

2.5 Standard Cleaning Process 1 and 2 (SC1 and SC2)

Standard cleaning processes 1 and 2, generally referred as SC1 and SC2 are used in industries to clean the substrate before starting to use it in the process. Silicon wafers, used for the photolithography process were cleaned with these processes before using them. Also after the wafers came back from deep reactive ion etching, the resist was stripped with acetone, methanol and DI water and then the wafers were cleaned using SC1 and SC2 processes. Both the processes are wet chemical cleaning processes. [7]

SC1 is used to remove any organic impurity that may be present on the substrate. The solution used is 6:1:1 (6 DI water: 1 NH_4OH: 1 H_2O_2). 6 parts of DI water and 1 part of ammonium hydroxide (NH_4OH) are mixed in a plastic petri dish and heated to 70±5°C. Then 1 part of hydrogen peroxide (H_2O_2) is added into the solution and then the substrate to be cleaned is put inside the solution. The substrate is cleaned for about 15 minutes and then rinsed with DI water bath.

SC2 is used to remove any metallic impurity that may be present on the substrate. The solution is 6:1:1 (6 DI water: 1 HCl: 1 H_2O_2). 6 parts of DI water and 1 part of hydrochloric acid (HCl) are mixed in a plastic petri dish and heated to 70±5°C. Then 1 part of hydrogen peroxide (H_2O_2) is added into the solution and then the substrate to be cleaned is put inside the solution. The substrate is cleaned for about 15 minutes and then rinsed with DI water bath.

CHAPTER 3: EXPERIMENTS AND RESULTS

In this chapter, the processes followed for the photolithography and kapton etching experiments are described and the results are discussed.

3.1 Photolithography Process with PR 4620 Positive Resist

The photolithography process deals with the following.

1. Resist thickness (15 ± 1 µm) determination experiments
   - Control Variable: Spin Speed and Spin Time
   - Response variable: Step height of photoresist
2. Bake time determination
   - Control variable: Hard bake time
   - Response variable: Hump height near the edge of upper diameter of valve pattern
3. Exposure time determination experiments
   - Control variable: Exposure time
   - Response variable: Upper and lower diameter of a valve pattern

3.1.1 Spin Speed and Time Variation

The main variables that control the resist thickness are spin speed and time. Since the desired thickness is as high as 15 µm, the AZ photoresist manufacturer suggested double coat method. In this method, the wafer is first coated with ~7.5 µm of resist. The resist is then

softbaked and then the wafer is coated with another layer of ~7.5 µm photoresist. This method is highly time consuming and also it was found out that when the wafer is coated with second layer of resist, the resist surface came out to be highly non uniform. As the PR4620 resist is very thick and takes long time to settle down, when the second layer is applied on the first layer of photoresist, and spun using the vacuum chuck, it could not spread out uniformly onto the wafer and gave a highly non uniform wavy surface. Hence it was decided to get the 15 µm thick resist on the wafer in a single run. It could be observed from Figure 2.6 that AZ PR4620 would give a thickness of close to 15 µm when spun with speed between 1000 – 1500 rpm. Different spin speeds 1000 rpm, 1200 rpm and 1500 rpm were used keeping all the other control variables constant and the thickness of the resist was measured. Spin time was kept 60 sec in order for the thick resist to spread evenly on the wafer. Pattern was developed and then measurements were taken using Veeco profilometer for the step height of the resist and were found out that spin speed of 1000 rpm for 60 sec would give the best result of 15 ±1 um.

Step measurements were done with Veeco profilometer using VSI mode. Symbols used to represent a variable are shown in Figure 3.1.

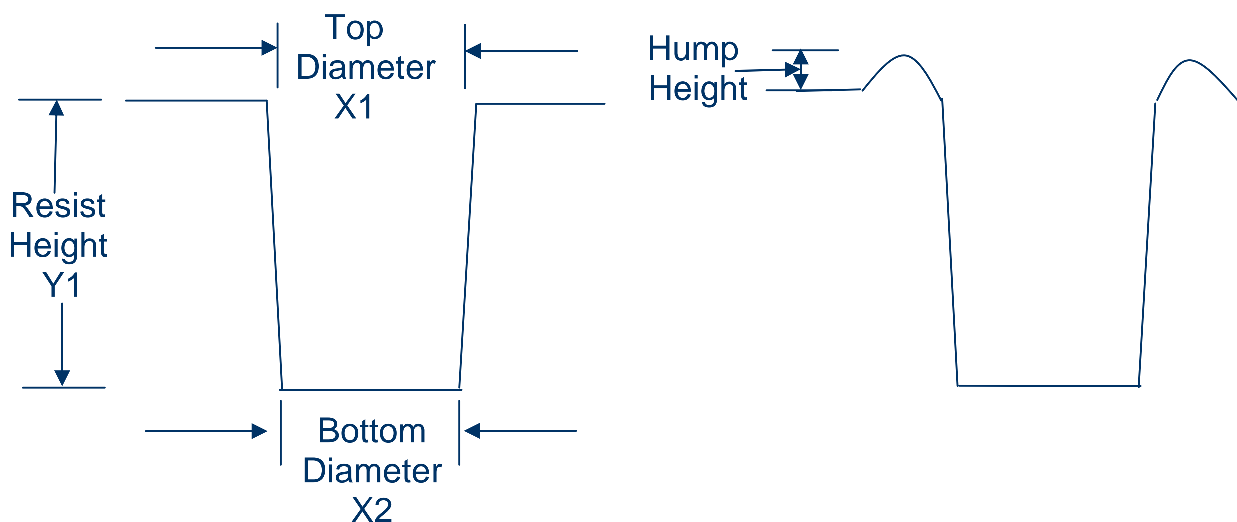

Figure 3.1 Parameters measured in photolithography process

X1 = Upper diameter of a valve pattern

X2 = Lower diameter of a valve pattern

Y1 = Step height of photoresist

Sidewall Profile = | X1 – X2| / 2. This indicates the slope of the tapered wall.

Average Hump Height = Hump present near the upper diameter edge of a valve pattern after hard bake

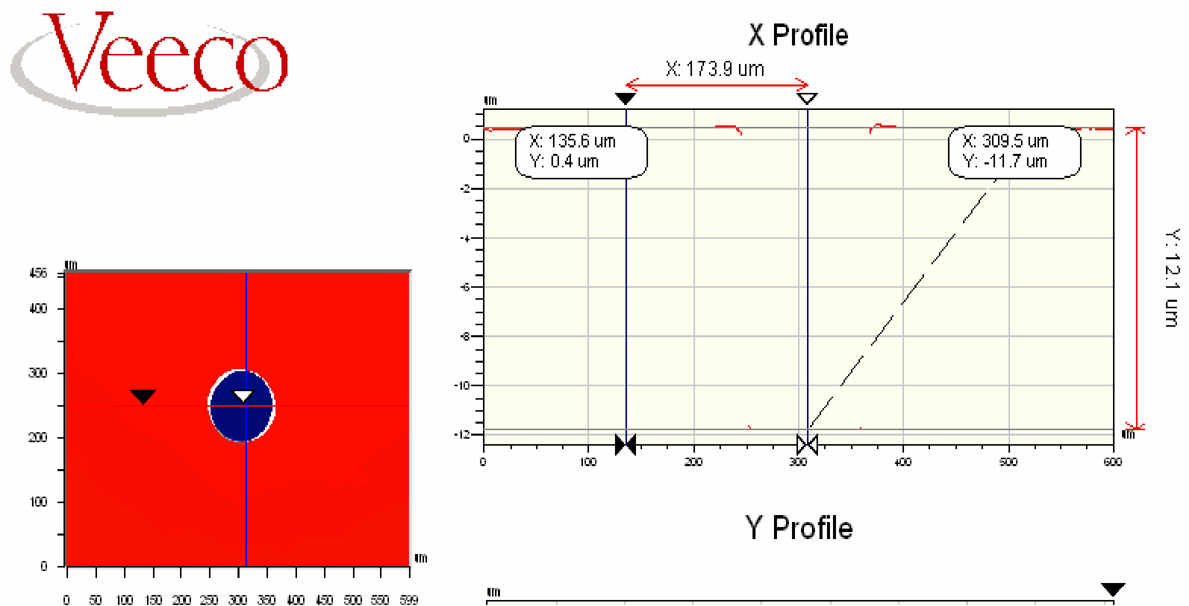

(a) Spin Speed: 1500 rpm, Spin Time: 60 sec

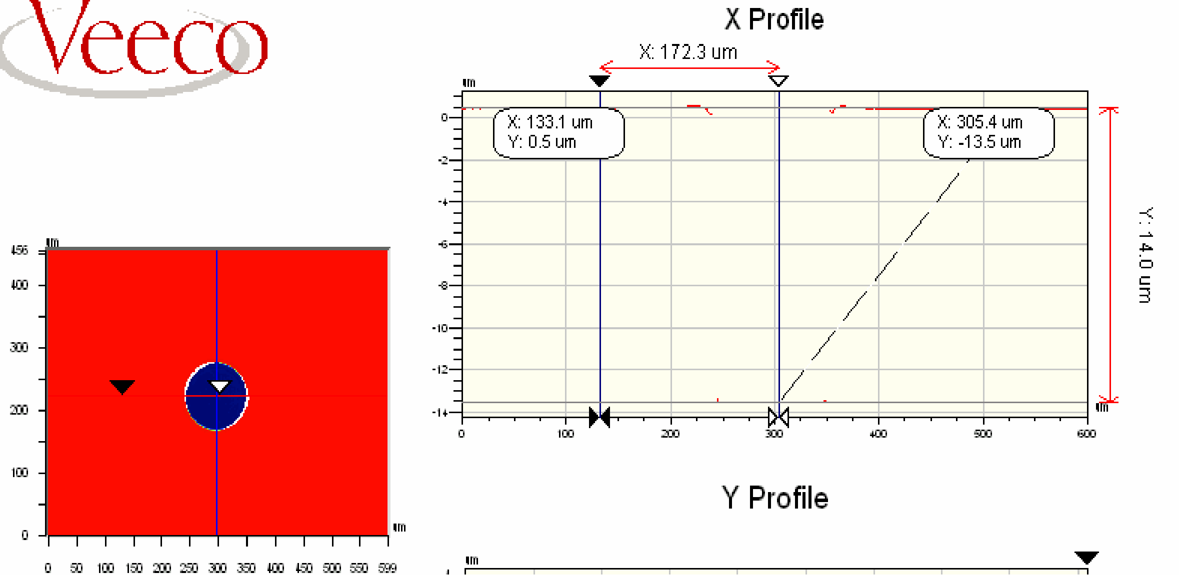

(b) Spin Speed: 1200 rpm, Spin Time: 60 sec

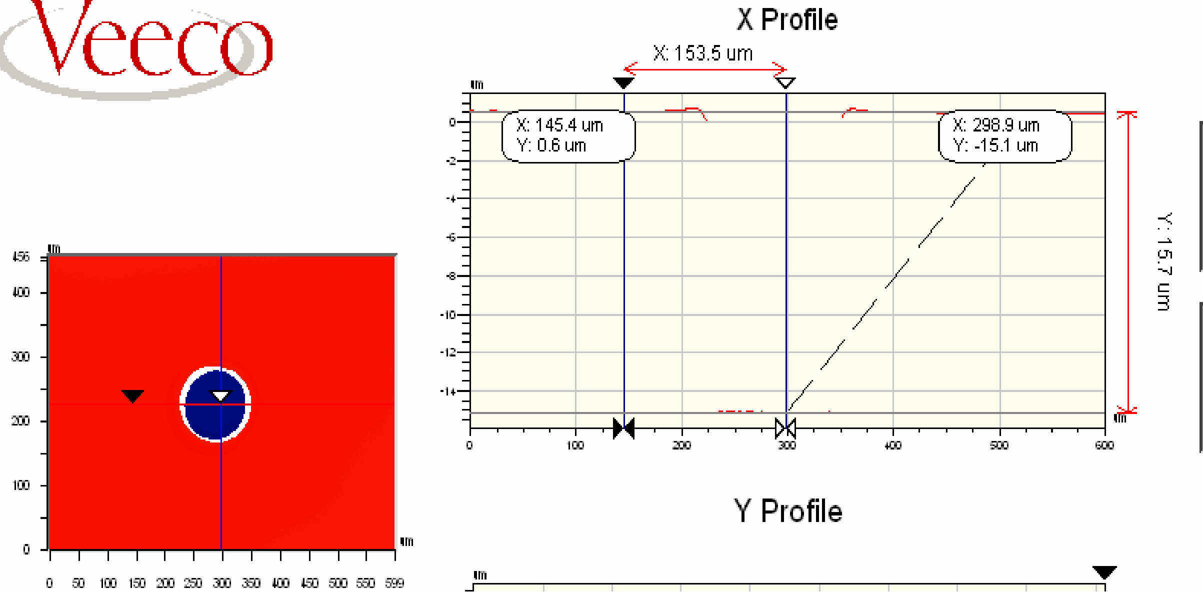

(c) Spin Speed: 1000 rpm, Spin Time: 60 sec

Figure 3.2 Veeco measurement for step height of photoresist

Figure3.2 (a), (b) and (c) shows the step height of a photoresist layer for the spin speeds of 1500, 1200 and 1000 rpm respectively. The image on the left hand side is the image result achieved by veeco profilometer. The red area is the photoresist surface and the blue circle is silicon surface. In order to measure the thickness of the photoresist, one cursor is placed on photoresist surface and another cursor is placed on the silicon surface. The height difference between these two points gives the thickness of resist. The measurements were taken in VSI mode, as the thickness of resist is in terms of micrometer. Table 3.1 shows the step height measurement results.

Table 3.1 Veeco measurement data for different spin speeds

Sample	**Spin Speed (rpm)**	Hole Dia (um)	Position on Wafer	**Y1 (um)**	X1 (um)	X2 (um)	Sidewall Profile (um)	Average Hump Height (um)
1	**1000**	100	Top	**15.6**	104.5	122.5	9	0.16
			Left	**15.9**	107	145.4	19.2	0.17
			Center	**15.7**	104.5	126.6	11.05	0.14
			Right	**15.1**	105.3	129	11.85	0.11
			Bottom	**15.6**	106.2	129	11.4	0.16
2	**1200**	100	Top	**13.6**	105.3	116.8	5.75	0.08
			Left	**13.4**	106.2	111.9	2.85	0.01
			Center	**14**	105.3	114.3	4.5	0.08
			Right	**13.4**	106.2	130.7	12.25	0.07
			Bottom	**13.7**	106.2	114.3	4.05	0.05
3	**1500**	100	Top	**12**	107	118.4	5.7	0.17
			Left	**11.9**	108.6	124.9	8.15	0.09
			Center	**12.2**	107	120.9	6.95	0.1
			Right	**12.3**	108.6	138	14.7	0.08
			Bottom	**12.5**	103.7	111.1	3.7	0.05

Figure 3.3 is a graphical representation of Table 3.1. Thus from Figure 3.2, 3.3 and Table 3.1, it is clearly seen that desired thickness of 15 µm is achieved if the resist is spun at the speed of 1000 rpm for 60 sec.

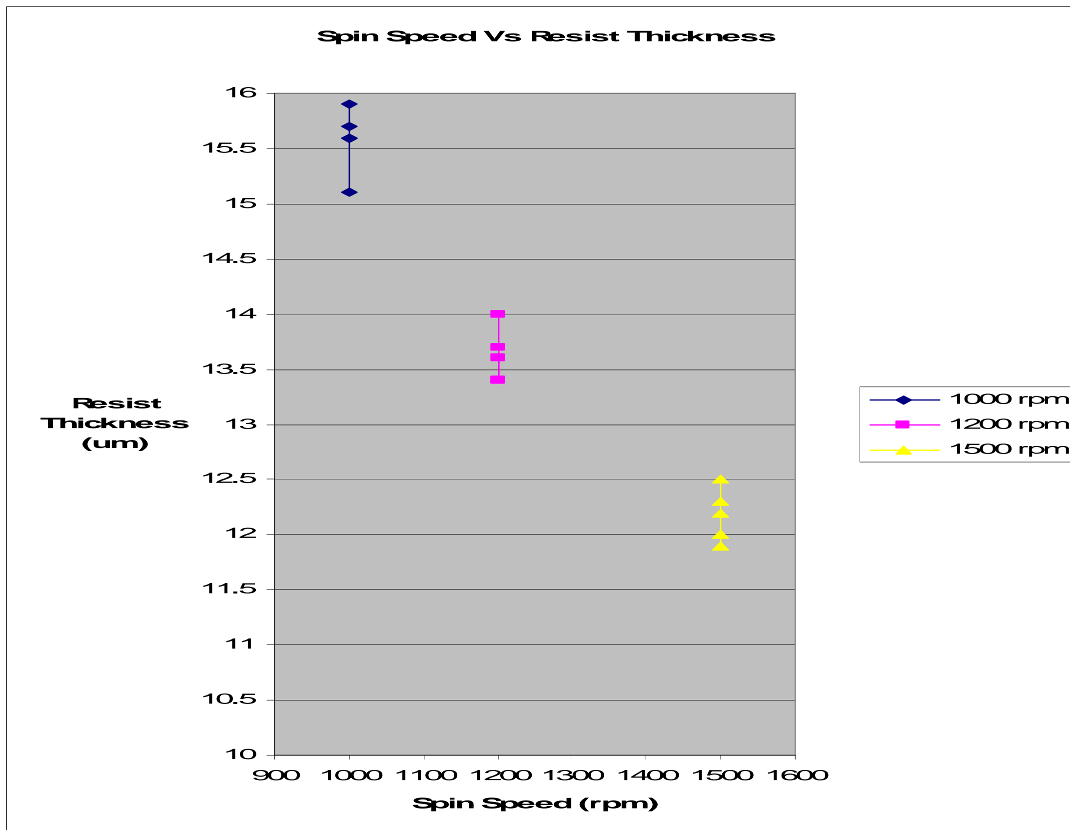

Figure 3.3 Spin speed vs. Resist thickness graph

3.1.2 Exposure Time Variation

Another critical parameter is the exposure time. The mask used is a dark field mask. If the positive resist is underexposed while using a dark field mask, the pattern diameter decreases than the original diameter and if the resist is over exposed, pattern diameter increases. Higher exposure time results in larger patterns. The resist was exposed for three different exposure time, 60 sec, 66 sec and 72 sec. Various experiments were carried out in order to determine the correct exposure time that would give the sidewall profile of not more than 6 µm.

Table 3.2 Veeco measurement data for different exposure time

Sample	**Exposure (sec)**	Hole Dia (um)	Position on Wafer	**X1 (um)**	**X2 (um)**	Y1 (um)	**Sidewall Profile (um)**	Avg. Hump Height (um)
1	**60**	100	Top	**96.4**	**109.4**	15.9	**6.5**	0.145
			Left	**106.2**	**120**	15.7	**6.9**	0.095
			Center	**99.6**	**109.4**	16.3	**4.9**	0.115
			Right	**103.7**	**117.6**	15.8	**6.95**	0.07
			Bottom	**101.3**	**110.2**	15.9	**4.45**	0.095
2	**66**	100	Top	**100.4**	**113.5**	15.7	**6.55**	0.05
			Left	**102.9**	**118.4**	15.6	**7.75**	0.13
			Center	**99.6**	**110.2**	17.5	**5.3**	0.105
			Right	**106.2**	**130.7**	15.7	**12.25**	0.13
			Bottom	**107**	**137.2**	15.7	**15.1**	0.17
3	**72**	100	Top	**100.4**	**111.1**	16.1	**5.35**	0.12
			Left	**106.2**	**123.3**	15.6	**8.55**	0.017
			Center	**108.6**	**129.8**	16.8	**10.6**	0.095
			Right	**104.5**	**137.2**	16.2	**16.35**	0.145
			Bottom	**98.8**	**108.6**	16	**4.9**	0.12

Table 3.2 clearly shows that 72 sec and 66 sec exposure time yield wider dimensions. The resist is over exposed with these exposure times and hence gives wider diameter resulting into higher sidewall profile. 60 sec exposure time yields a sidewall profile in the tolerance limit of 6 µm. 54 sec exposure time was also tried but it resulted into no development of the resist. Figure 3.3, Figure 3.4 and Figure 3.5 shows one point measurement for 72 sec, 66 sec and 60 sec exposure time respectively. Figure 3.6 illustrates the data of Table 3.2 in a chart format. It can be observed that 66 sec and 72 sec exposure times give sidewall profiles that range from 4.9 µm to 16 µm. On the other hand, 60 sec exposure time yield uniform sidewall profile in the range of 4.5 µm to 6.5 µm.

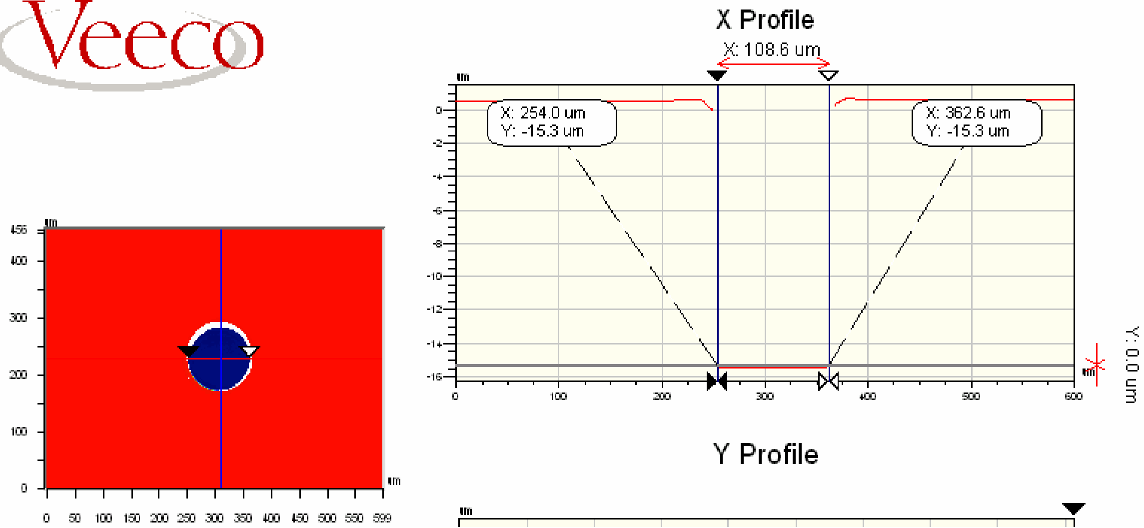

(a): 72 sec exposure - Bottom diameter

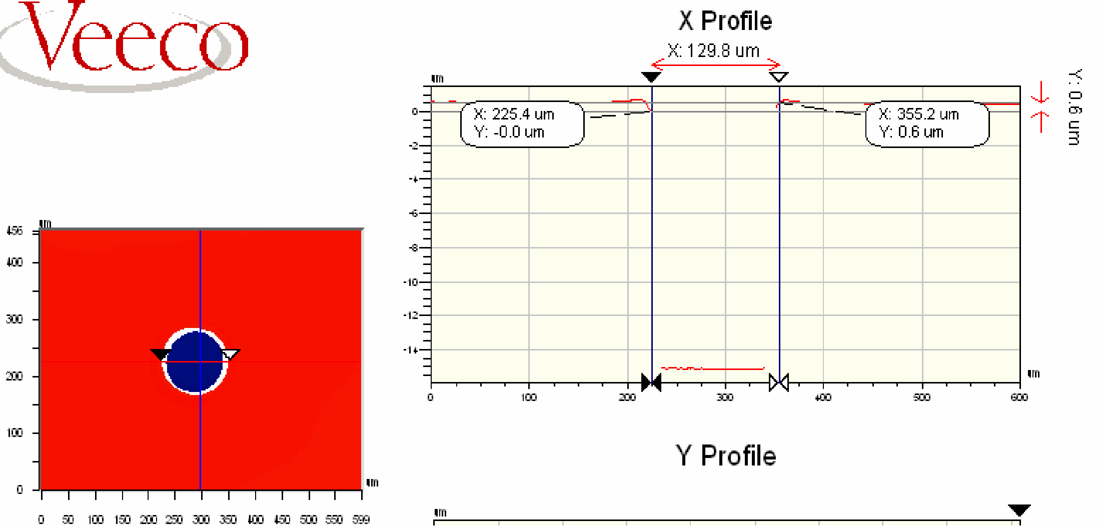

(b): 72 sec exposure - Top diameter

Figure 3.4 Pattern diameter measurement for 72 sec exposure time

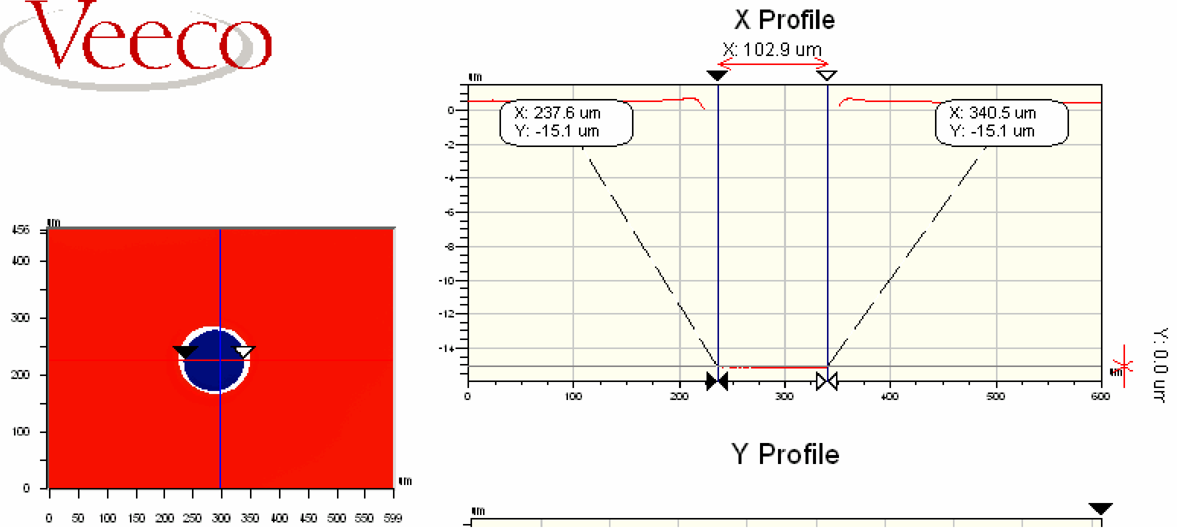

(a): 66 sec exposure - Bottom diameter

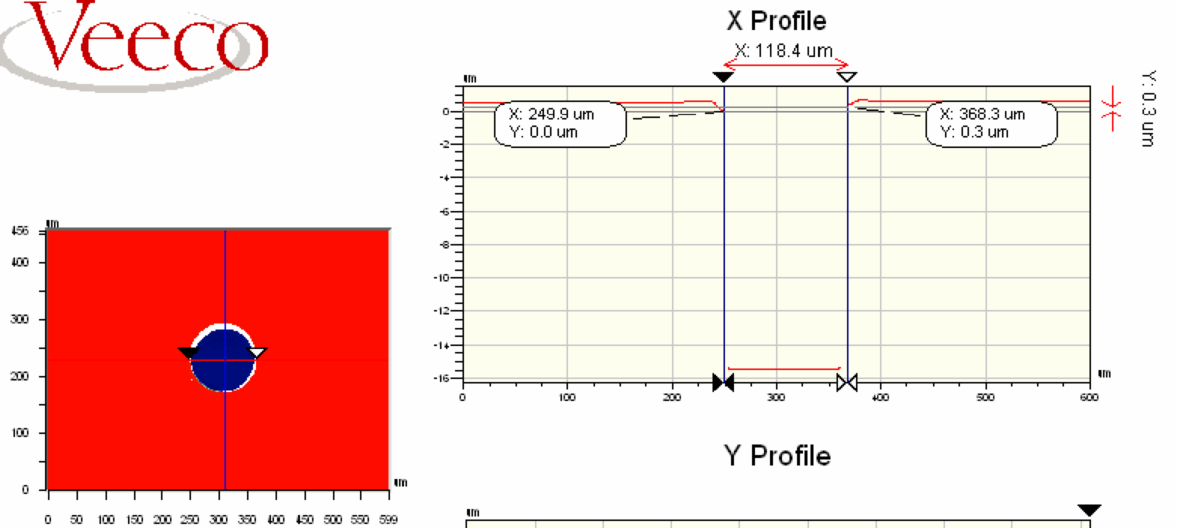

(b): 66 sec exposure - Top diameter

Figure 3.5 Pattern diameter measurement for 66 sec exposure time

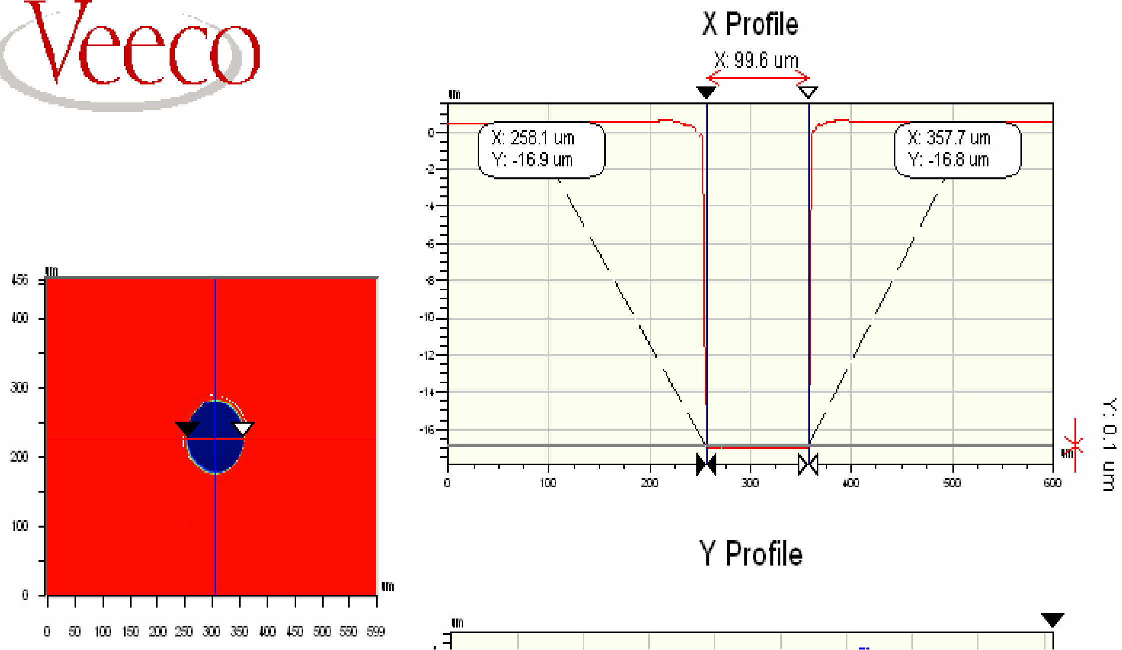

(a): 60 sec exposure – Bottom diameter

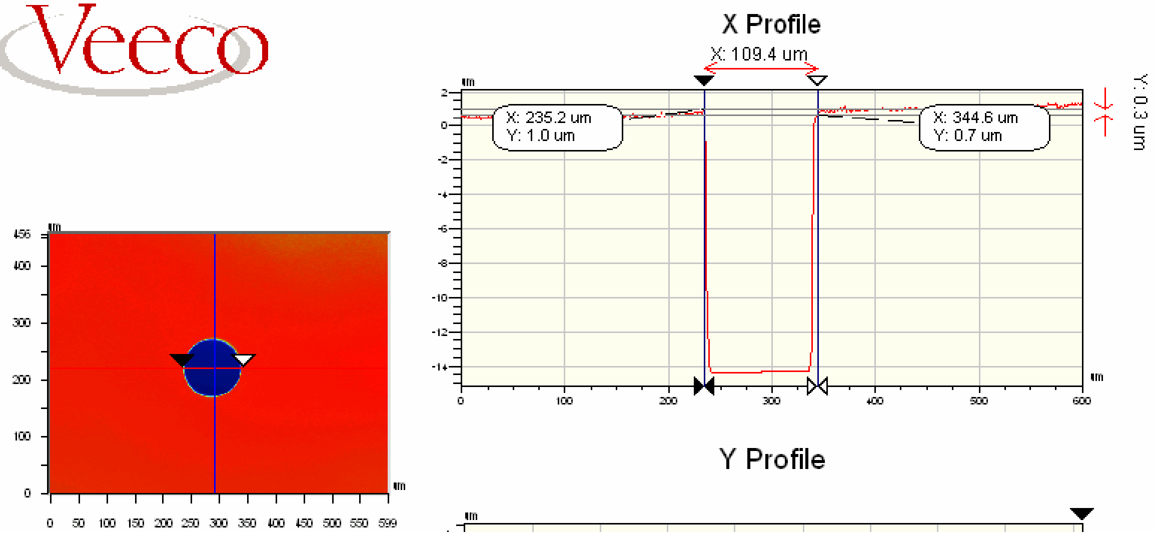

(b): 60 sec exposure – Top diameter

Figure 3.6 Pattern diameter measurement for 60 sec exposure time

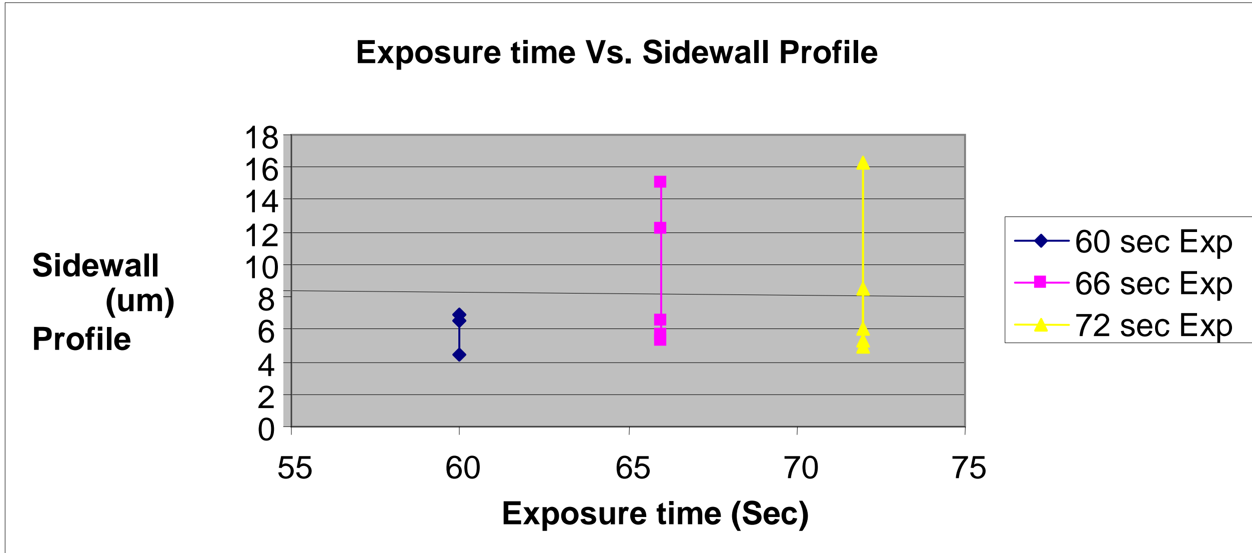

Figure 3.7 Exposure time vs. sidewall profile graph

3.1.3 Bake Time Variation

After the spin speed and time are determined which give the desired thickness, and the exposure time is determined which gives the desired dimensions, the next step was taken to determine the correct hard bake time. If the hard bake time is shorter than required time the resist would not bake completely which would affect the DRIE as the resist would still be in semi liquid form. On the other hand if hard bake time is more than required then the resist would shrink resulting in wider patterns. Also it was noticed that for the longer hard bake time, a hump was developed near the step. The correct dimensions of the pattern also depend on the exposure time. Longer exposure time results in wider patterns. So, the hard bake time is finalized based on the lowest hump height achieved.

Three different hard bake time, 15 min, 10 min and 5 min were used in order to study the effect on hump height. Hardbake temperature was kept constant at 90°C as suggested by the AZ resist datasheet. Results of average hump height achieved are shown in Table 3.3.

Table 3.3 Effect of hard bake time on hump height

Sample	Hardbake time (min)	Hole Dia (um)	X1 (um)	X2 (um)	Sidewall Profile (um)	Avg. Hump Height (um)
1	15	100	84.1	164.1	40	0.2335
2	10	100	99.6	157.6	58	0.1015
3	5	100	108.6	138	29.4	0.024

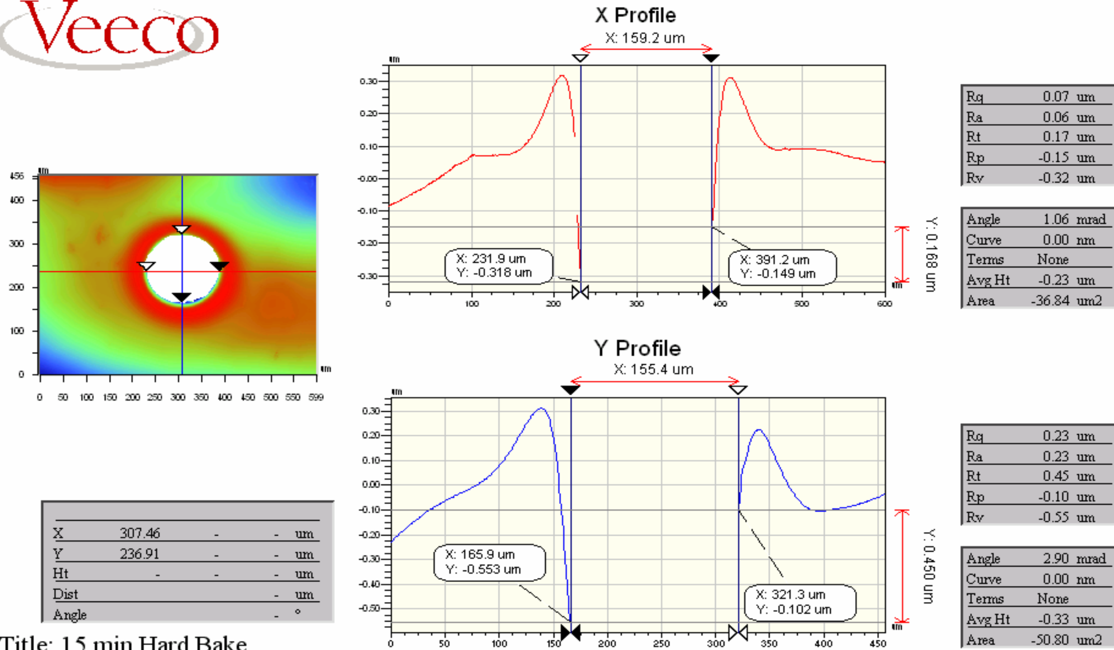

Figure 3.8 Hump created with hard bake time 15 min

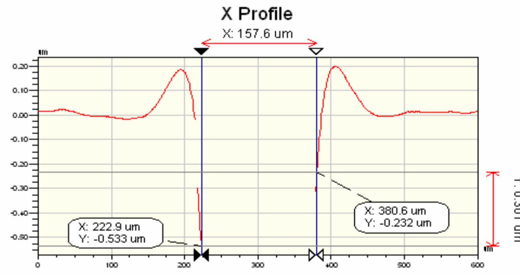

Rq	0.12	um
Ra	0.10	um
Rt	0.30	um
Rp	-0.23	um
Rv	-0.53	um

Angle	1.91	mrad
Curve	0.00	nm
Terms	None	
Avg Ht	-0.34	um
Area	-53.03	um2

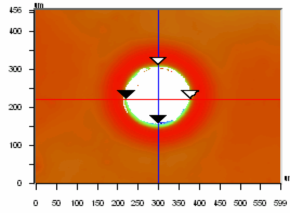

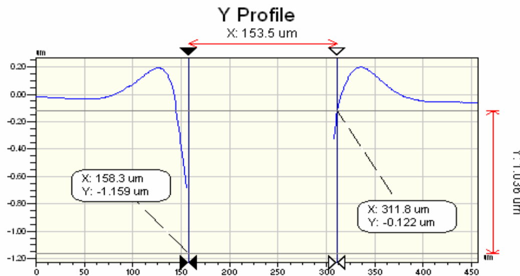

Rq	0.36	um
Ra	0.26	um
Rt	1.04	um
Rp	-0.12	um
Rv	-1.16	um

Angle	6.77	mrad
Curve	0.00	nm
Terms	None	
Avg Ht	-0.37	um
Area	-57.29	um2

X	300.12	-	-	um
Y	221.69	-	-	um
Ht	-	-	-	um
Dist			-	um
Angle			-	°

Title: 10min Hard Bake

Note:

Figure 3.9 Hump created with the hard bake time 10 min

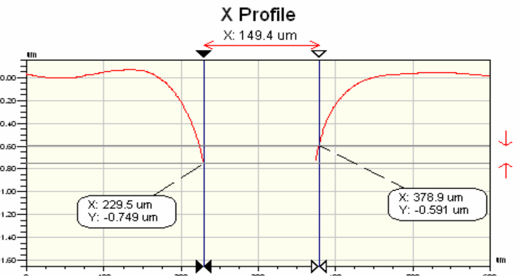

Rq	0.30	um
Ra	0.23	um
Rt	0.98	um
Rp	-0.59	um
Rv	-1.57	um

Angle	1.06	mrad
Curve	0.00	nm
Terms	None	
Avg Ht	-0.81	um
Area	-121.04	um2

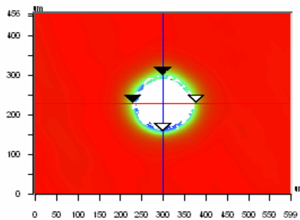

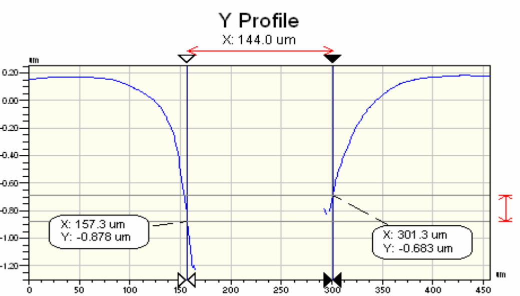

Rq	0.19	um
Ra	0.17	um
Rt	0.55	um
Rp	-0.68	um
Rv	-1.23	um

Angle	1.35	mrad
Curve	2.57	mm
Terms	None	
Avg Ht	-0.95	um
Area	-137.03	um2

X	300.12	-	-	um
Y	229.30	-	-	um
Ht	-	-	-	um
Dist			-	um
Angle			-	°

Title: 5 min Hard Bake

Note:

Figure 3.10 Hump created with hard bake time 5 min

Figure 3.8 shows Veeco measurement for the hump height when hard bake time is 15 min. Figure 3.9 and 3.10 shows the measurement result for the hard bake time of 10 min and 5 min respectively. It could be observed from various runs of experiments that the hard bake time of 5 min gives desired results with no significant hump present near the edges of the pattern. Table 3.3 shows the average of all the data measured for hum height. It is observed from the data that hard bake time of 5 min does not create any significant hump.

Once the three parameters, spin speed, exposure time and hard bake time, are determined, the wafers were then prepared and sent for DRIE. After the wafers were etched, the resist was stripped using acetone, methanol and DI water. The wafer was then cleaned using SC1 and SC2 process. Veeco measurements were taken for the etched pattern. The result showed that etching on the front side of the wafer gave results close to the actual diameter but the dimension on the back side was almost double than the actual diameter.

Table 3.4 Post DRIE measurement

Hole Dia (um)	Position on Wafer	Front x1 (um)	Back x2 (um)	|x2-x1| (um)
100	Top	180.5	102.9	77.6
	Center	187	102.9	84.1
	Left	193.5	103.7	89.8
	Right	171.5	103.7	67.8
	Bottom	203.3	102.9	100.4

3.2 Kapton Etching Methodology

Wet etching is purely a chemical process that can be isotropic in amorphous materials such as silicon dioxide and directional in crystalline materials such as silicon. Contaminants and particulates in this type of process are purely a function of the chemical purity or of chemical system cleanliness. Agitation of the wet chemical bath is frequently used to aid the movement of reactants and by-products to and from the surface. Agitation will also aid the uniformity of etch, since the by products may be in the form of solids or gases that must be removed. A modern wet-chemical bench will usually have agitation, temperature and time controls as well as filtration to remove particulates. [14]

In this experiment HN type Kapton is used. The purpose of the experiment is to establish a uniformly blanket etch process for Kapton film. The thickness of the film is 125 µm. The purpose is to etch 25 µm of Kapton uniformly and obtain a 100 µm film with good roughness measures.

Experiment Response Variables

- Etch rate
- Concentration of solution
- Surface roughness of Kapton film

Experiment Control Variables

- Etch time
- Temperature of the etching solution

3.2.1 Procedures for Kapton Etching

Dupont suggested that 32 grams of KOH dissolved in 400 grams of ethanol and 100 grams of water, heated to 70°C would etch Kapton at the rate of 10µm/min. This experiment was first carried out, but after 2 minutes of etching, kapton piece became like a molten rubber piece. In place of ethanol we used Isopropyle Alcohol was used [11].

KOH = 16 grams

IPA = 200 grams

Now, 0.79 grams of IPA = 1 ml of IPA

So, 200 grams of IPA ~ 250 ml of IPA

DI WATER = 50 grams

Now, 1 gram of DI Water = 1 ml of DI Water

So, 50 grams of DI Water = 50 ml of DI Water

Thus 16 grams of KOH, 250 ml of IPA and 50 ml of DI water used as etching solution. In order to obtain desired post etch surface roughness and etch rate, different concentrations of KOH, IPA and DI water were taken to prepare an etching solution as shown in Table 3.6. Kapton samples were cut in 1 cm x 1 cm pieces. Thickness of the sample before etch is 125 µm. Average surface roughness, (R_a) and peak-to-valley (R_t) roughness were measured at five locations on each sample before etching using Veeco profilometer.

Table 3.5 Roughness measurement on the smooth and rough side of the Kapton piece before etching

Rough side	Ra (nm)	Rt (um)		Smooth side	Ra (nm)	Rt (um)
Pt1	302.38	1.98		Pt1	192.23	2.57
Pt2	277	1.68		Pt2	167.93	1.67
Pt3	315.36	2.09		Pt3	169.14	3.62
Pt4	268.59	1.77		Pt4	180.58	3.41
Pt5	283.5	1.76		Pt5	177.35	1.62
Average	276.045	1.765		Average	178.965	2.515

Also sample thickness was measured at five different locations using micrometer. It was found to be uniform 5 mil (125 μm).

The etch solution was prepared as shown in Table 3.6 and initial pH of the unheated solution was measured and recorded.

Table 3.6 Etching solution concentration for Kapton etching

Exp No.	KOH (gm)	IPA (ml)	DI WATER (ml)	Initial pH
1	10	250	50	14
2	10	250	100	14
3	10	300	50	14
4	10	300	100	14
5	13	275	75	14
6	16	250	50	14
7	16	250	100	14
8	16	300	50	14
9	16	300	100	14

Each experiment was carried out separately. Etching solution was made in a 500 ml size glass beaker. When the KOH was fully dissolved in DI Water and IPA, small amount of solution ~ 50 ml was transferred into a 200 ml size glass beaker which was then put for

heating on the hot plate. The IPA starts evaporating and this may change the concentration of the solution, so in order to make sure that the initial pH of the etchant remains same during and after etching, pH is measured. The beaker is kept covered with a glass lid. The etchant should reach 70°C before the sample is put for etching.

The etching solution should not be boiled; hence the temperature is constantly monitored with a thermometer. The time for the etching solution to reach 70°C from room temperature is measured using stop watch. This time is normally 20 min. Also the time required for the heated etching solution to stabilize at 70°C is recorded, which is not more than 7-8 min. After the etchant temperature is stabilized at 70°C, one Kapton sample is immersed in the etchant for 5 minutes. After 5 minutes the sample is removed from the etchant and placed in DI water rinse bath for 5 minutes. The etching solution is constantly stirred with a Teflon rod during etching process. The etching solution temperature is recorded and a new Kapton sample is immersed in the solution immediately. After 5 minutes the sample is removed from the etching solution and placed in an overflowing DI water rinse. The hot plate is then turned off and the beaker with the etching solution is moved to safe surface in the hood. Etching solution pH is measured again. After the DI water rinse bath for 5 minutes, the samples are blow dried with an N_2 gun. It is important to note that no heat should be used on the etched sample. Thickness of the etched sample is measured at five different points to determine the etch rate and then surface roughness, R_a and R_t are measured of all samples at five locations as in the pre-etch measurement step. Kapton itself is not a reflective material and after etching it becomes difficult to measure the roughness with Veeco, so a very thin layer (100 Å) is deposited on all the samples both on front and back sides and then the roughness measurements are done.

3.2.2 Post Etch Results

Various measurements were taken to determine the roughness of the film after etching and to select the process that is best suitable for the desired results. Terminologies used to identify the variables are listed below.

X1 = Pre etch kapton film thickness

X2 = Post etch kapton film thickness

1 mil = 25 µm

Etch time = 5 min

Etching temperature = 70°C

Delta Thickness = Pre etch thickness (X1) – Post etch thickness (X2)

Etch rate = Delta Thickness (µm) / 5 min

Table 3.7 shows the pre and post etch thickness measurements of the Kapton film. Based on the thickness measurement etch rate can be found out by dividing the etched thickness with the etch time, which is 5 min in this experiment. Negative etch rate, in case of experiment no. 2 and 4 shows that the kapton film after etching got swollen and did not give a desired etching. Also it can be seen that the etch rate varies as the etchant concentration changes.

Table 3.7 Experiment Results: Etch rate measurement

Exp No.	Sample No.	Pre-etch X1 (mil)	Post-etch X2 (mil)	Delta Thickness X1-X2 (mil)	Delta Thickness X1-X2 (µm)	Calculated Etch Rate (µm/min)	Average Etch rate (µm/min)
1	1	5	4.6	0.4	10	2	
	2	5	4.52	0.48	12	2.4	2.13
	3	5	4.6	0.4	10	2	
2	1	5	5.08	-0.08	-2	-0.4	
	2	5	5.58	-0.58	-14.5	-2.9	-1.96
	3	5.02	5.54	-0.52	-13	-2.6	
3	1	5	4.58	0.42	10.5	2.1	
	2	5.02	4.5	0.52	13	2.6	1.7
	3	5.02	4.94	0.08	2	0.4	
4	1	5	5.38	-0.38	-9.5	-1.9	
	2	5	5.2	-0.2	-5	-1	-1.16
	3	5	5.12	-0.12	-3	-0.6	
5	1	5	4.44	0.56	14	2.8	
	2	5	4.4	0.6	15	3	2.93
	3	5	4.4	0.6	15	3	
6	1	5	4.3	0.7	17.5	3.5	
	2	5	4.26	0.74	18.5	3.7	3.7
	3	5	4.22	0.78	19.5	3.9	
7	1	5	4.44	0.56	14	2.8	
	2	5.02	4.5	0.52	13	2.6	2.76
	3	5	4.42	0.58	14.5	2.9	
8	1	5	4.22	0.78	19.5	3.9	
	2	5	4.2	0.8	20	4	4.1
	3	5	4.12	0.88	22	4.4	
9	1	5	4.48	0.52	13	2.6	
	2	5	4.5	0.5	12.5	2.5	2.6
	3	5	4.46	0.54	13.5	2.7	

Table 3.8 shows the average roughness obtained for each run. From the results, it can be observed that experiment 7 and 9 yield lowest roughness among all the experiments. The etch rate also needs to be studied in order to determine the process that yields optimum roughness and etch rate.

Table 3.8 Average Etch rate and surface roughness results

Exp	KOH (gm)	IPA (ml)	DI WATER (ml)	Etch Time (sec)	Etch Rate (um/min)	Roughness (um)
1	10	250	50	5	2.13	348.24
2	10	250	100	5	-1.96	406.41
3	10	300	50	5	1.7	191.92
4	10	300	100	5	-1.16	206.27
5	13	275	75	5	2.93	169.98
6	16	250	50	5	3.72	382.67
7	16	250	100	5	2.76	152.64
8	16	300	50	5	4.1	167.45
9	16	300	100	5	2.6	118.25

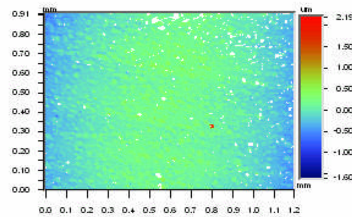

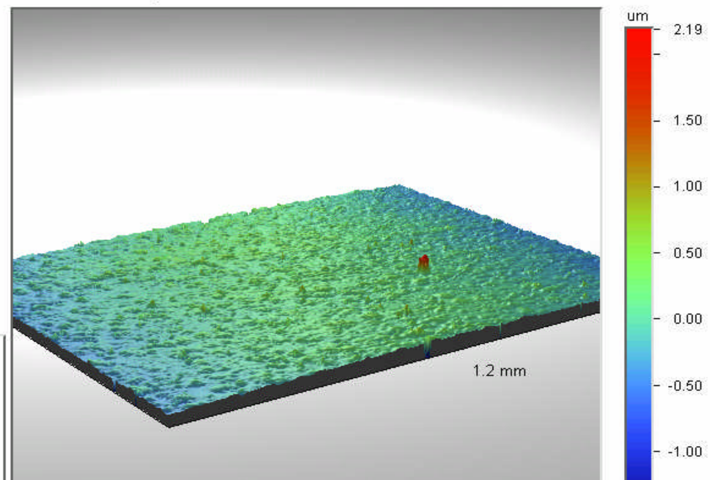

Figure 3.11 Pre Etch surface roughness measurement on one sample

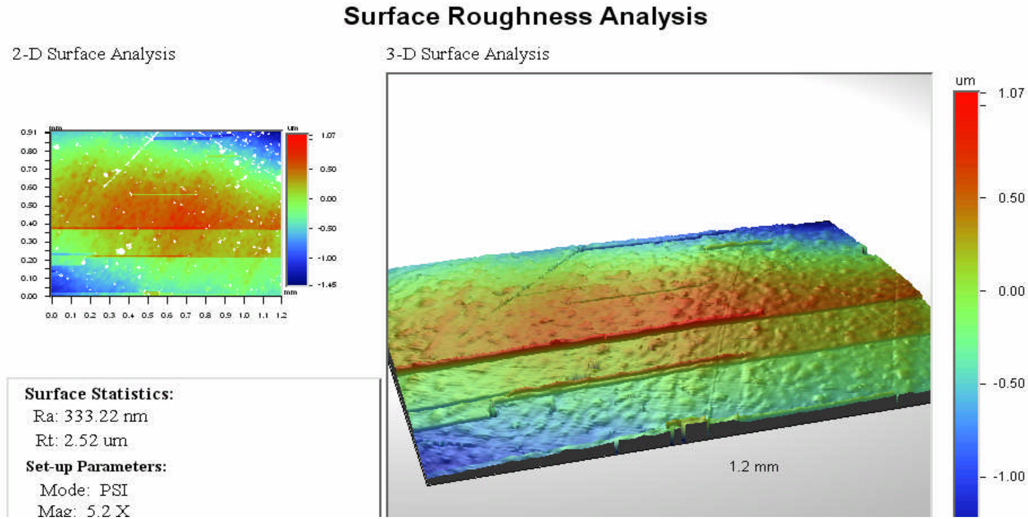

Figure 3.12 Post etch surface roughness measurement on one sample

Figure 3.11 and 3.12 show measurement on the pre and post etched sample. It can be observed that after etching, surface roughness of the sample gets affected.

3.2.3 Surface Roughness and Etch Rate Measurement

Initial thickness (X1) of the film is measured at five different points using micrometer. After etching the thickness (X2) is measured again at five different points using micrometer. The etch rate is measured by taking the difference (Delta) between the initial thickness (X1) and post etch thickness (X2) of the film and then dividing the difference by the etch time which is 5 min in this case. The etch rate is defined in terms of micrometer per minute.

As seen in Figure 3.13 the etch rate for experiment number 2 and 4 is negative. This indicates that instead of getting etched, the film got swollen after etching. This shows that higher concentration of DI water with lower concentration of KOH does not etch the Kapton film uniformly but it transforms the film into a molten rubber form which accounts for the greater film thickness after etching.

After determining which experiments give positive etch rate, the next step is to determine the fastest etch rate that gives smoother surface roughness.

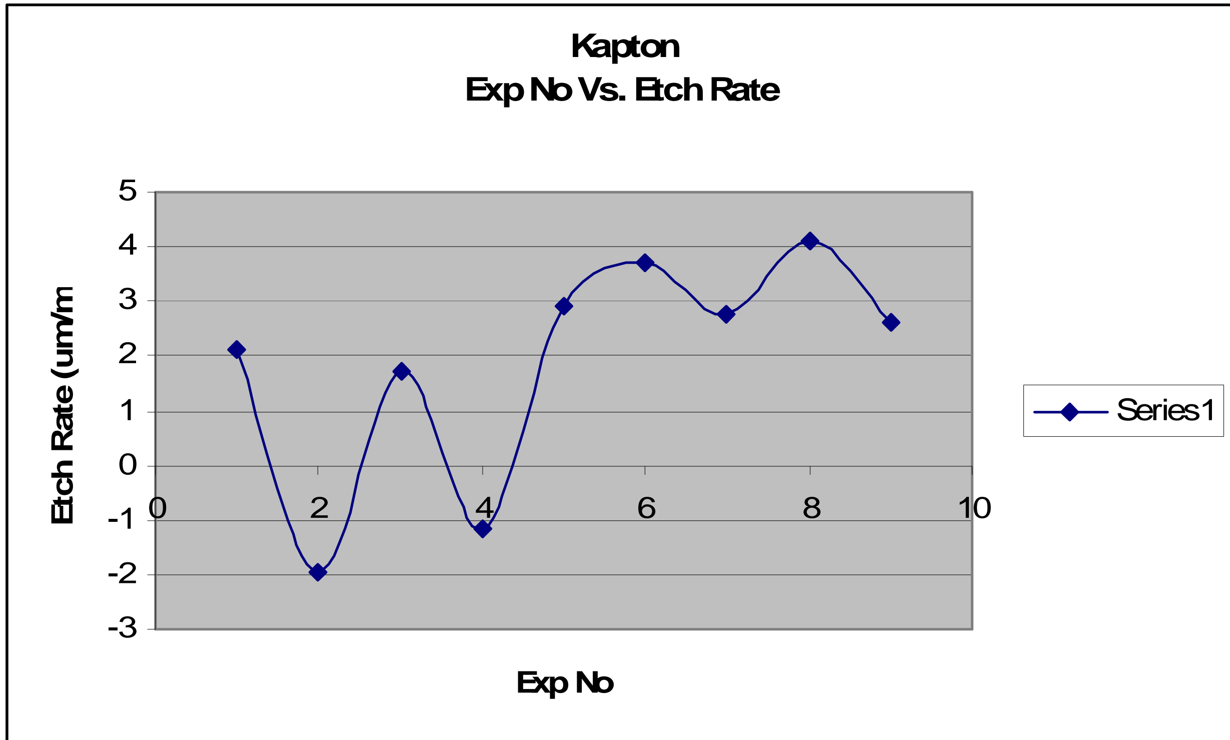

Figure 3.13 Etch rate curve for kapton

Table 3.9 Comparison of results

Exp	KOH (gm)	IPA (ml)	DI WATER (ml)	Etch Time (sec)	Etch Rate (µm/min)	Roughness (µm)
3	10	300	50	5	1.7	191.92
5	13	275	75	5	2.93	169.98
7	16	250	100	5	2.76	152.64
8	16	300	50	5	4.1	167.45
9	16	300	100	5	2.6	118.25

Table 3.9 lists extracted data from Table 3.8. All the negative results and results with high post etch roughness are removed from Table 3.8 and the remaining results are shown in Table 3.9. It can be observed that experiment no. 3,5,7,8 and 9 give desirable results. Any one of these five experiments can be used to obtain the desired results. But it is clearly seen that the etch rate of experiment 3 is lowest and the roughness after etching is also highest among these five batches. So the etching solution concentration of experiment 3 is not used as final etch process. Also it is clearly observed that lower concentration of KOH does not give smoother surface roughness after etching and it also lowers the etch rate. Also it is noticed from experiment 7 and 9 that 16 gms of KOH and 100 ml of DI water give smoother surface roughness result and the etch rate is also satisfactory.

CHAPTER 4: CONCLUSION

Experiments were carried out in order to obtain a photolithography process that builds 15 µm thick resist mask on 3 inch silicon wafer and to develop a wet etch process for etching of kapton polyamide film. Measurements were taken with the Veeco profilometer, which gave highly accurate measurements.

For the photolithography process, resist thickness and critical dimensions of the pattern were two areas of concern. Experiments were carried using different spin speeds, in order to achieve the desired thickness of 15 µm. Characteristics of the photoresist AZ PR4620 were studied from the data sheet and it could be determined that spin speed in the range of 1000 rpm to 1500 could give the desired thickness of 15 µm. Various experiments were carried out and resist was spun at 3 different spin speeds of 1000 rpm, 1200 rpm and 1500 rpm. For each run, a pattern was developed on the wafer and then veeco profilometer was used to measure the step height of the resist. Spin speed of 1000 rpm gave the desired result. Exposure time play a key role in obtaining the critical dimensions of the pattern. For the positive resist, if the resist is overexposed, the pattern would have wider dimensions than the original. Hence exposure time has to be closely selected. Manufacturer recommendation of 90 sec exposure time was found to be very high and resulted in having dimensions almost double than the original size. Three different exposure times were selected, 72 sec, 66 sec and 60 sec. Results showed that 60 sec exposure time gave the best result. Measurements were taken on each side of the wafer. As the wafer is 3 inch in diameter, it was very important that the results obtained for each experiment were uniform on all the different sides of the wafer. The thickness of the resist and dimensions of the pattern should not vary when moved from center to near the edges of the wafer. Considering

this aspect, the exposure time of 60 sec gave the most uniform results as opposed to other exposure time. Also in order to get a uniform thickness of 15 µm, the wafer should be placed on the vacuum chuck in such a way that it does not wobble while spinning. Third critical parameter, hard bake time, was determined based on the hump achieved at the edge of the pattern. The photoresist mask was built on silicon wafer for DRIE. The pattern on the resist had to be etched in silicon. Thus any hump present near the pattern would affect the deep reactive ion etching and the wafer would not etch in a desired way. Out of three different hard bake time used, 5 min of hard bake time gave no hump at the edge of the pattern. Thus it was determined that in order to develop a 15 µm thick layer of AZ 4620 resist, the spin speed should be 1000 rpm for 60 sec spin time, exposure time should be 60 sec and hard bake time should be 5 min at 90 °C in oven. Soft bake should be done for 1 min at 70°C and 5 min at 90°C on hot plates.

Wet etch technique for a polyamide material is a difficult process as the material tend to obtain a molten rubber like property at high temperatures with higher DI water content. Kapton polyamide film had to be etched uniformly and the post etch roughness was a critical response variable. Different concentrations of KOH, IPA and DI water were mixed and the etching solution was heated to 70°C. Kapton film absorbs moisture, so if the DI water concentration was kept high, the film started absorbing the water content and became a molten rubber like piece. It was clearly observed that lower concentration of KOH did not give smoother surface roughness after etching and it also lowered the etch rate. Also it was noticed from experiment 7 and 9 that 16 gms of KOH and 100 ml of DI water gave smoother surface roughness result and the etch rate was also satisfactory. With the etch rate obtained, 25 µm of kapton could be etched in 11 to 12 minutes at 70°C

Thus two of the main processes involved in fabricating an electrostatic valve were successfully developed. For the future work, DRIE results can be studied in detail and based on

the results some changes in resist bake time and temperature can be made to achieve the desired result after deep reactive ion etching. For wet chemical etching of kapton, etching temperature can be varied. Variation in temperature will affect the etch rate, and hence faster etch rate can be achieved. Also in the above experiments, kapton pieces were immersed in etching solution while etching. If the etching solution is sprayed instead, highly smooth surface can be achieved.

LIST OF REFERENCES

1. Edward K. Chan, Robert W. Dutton, " Electrostatic micromechanical actuator with extended range of travel", IEEE Volume 9, Issue 3, September 2000
2. Juan Pablo Saenz, Study of processes and materials of MEMS integration with cryogenic devices, MS Thesis, 2003
3. Mitsuhiro Shikida, Kazuo Satoand, Takeshi Harada, " Fabrication of an S shape microactuator", IEEE Volume 6, March 1997
4. Mitsuhiro Shikida, Kazuo Sato, Shinji Tanaka, Yoshio Kawamura, Yoshihisa Fujisaki, " Electrostatically driven gas valve with high conductance", Volume 3, Issue 2, June 1994
5. Raviprakash Peelamedu, Effect of deposition temperature and post deposition annealing on the electrical properties of BST capacitors, Thesis UCF 2004
6. Richard Jaeger, Introduction to microelectronic fabrication
7. University of Central Florida Laboratory manual
8. Positive resist AZ 4000 series data sheet
9. Positive resist developer AZ 400K data sheet
10. Mohamed Gad-el-Hak, The MEMS handbook
11. Dupont
12. Veeco profilometer handbook
13. Jerry Sergent and Charles Harper, Hybrid microelectronics handbook
14. Michael Kohler, Etching in Microsystem Technology